P-07-165

Forsmark site investigation

Transient electromagnetic soundings at Forsmark and the regional surroundings

Estimations of depth to saline groundwater

Hans Thunehed, Timo Pitkänen
GeoVista AB

September 2007

Svensk Kärnbränslehantering AB
Swedish Nuclear Fuel
and Waste Management Co
Box 5864
SE-102 40 Stockholm Sweden
Tel 08-459 84 00
+46 8 459 84 00
Fax 08-661 57 19
+46 8 661 57 19

ISSN 1651-4416
SKB P-07-165

Forsmark site investigation

Transient electromagnetic soundings at Forsmark and the regional surroundings

Estimations of depth to saline groundwater

Hans Thunehed, Timo Pitkänen
GeoVista AB

September 2007

Keywords: Forsmark, AP PF 400-06-118, TEM, Resistivity, Saline groundwater.

Abstract

Seven transient electromagnetic (TEM) soundings have been performed at the site investigation area at Forsmark and further towards south and west. The data were in most cases compatible with layered earth models and the data were therefore inverted into a constrained four-layer model at each station.

The results from sounding stations away from the Baltic Sea have a different character compared to the results from stations inside or close to the site investigation area. The former indicate high-resistivity near-surface rock (> 10,000 Ωm) underlain by rocks of moderate resistivity (~ 3,000 Ωm), at depths ranging from 600 to 1,500 metres. The high-resistivity rocks are only present at shallow depths in the site investigation area. The moderate resistivity rocks can here be found close to the surface. Low-resistivity rock (500 to 1,000 Ωm) is indicated at a depth of around 700 to 1,100 metres in the site investigation area.

The data quality varied between the soundings. All soundings were affected by cultural noise, but all except two gave reliable inversion results. The error bounds for the layer parameters are however fairly large, especially for the resistivity of the layers. It should also be realized that the actual resistivity structure in the ground is not expected to be in the form of discrete layers. Instead a gradual decrease in resistivity is expected with increasing depth.

The variation of resistivity with depth is interpreted to be due to an increase in salinity. Other factors, such as lithology, porosity and fracturing, are expected to be of no major importance. However, two-dimensional structures have affected the data. This is most evident for a sounding station that is located close to the regional Forsmark deformation zone.

Sammanfattning

Sju transienta elektromagnetiska sonderingar har utförts vid platsundersökningsområdet i Forsmark och vidare mot syd och väst. Mätdata var i de flesta fall kompatibla med en horisontellt lagrad jordmodell och data inverterades därför till en styrd fyrlagermodell för varje station.

Resultaten för sonderingsstationer en bit ifrån havet har en annorlunda karaktär jämfört med stationer i och nära platsundersökningsområdet. De förra indikerar högresistivt berg nära ytan (> 10 000 Ωm) som underlagras av berg med mera moderat resistivitet (~ 3 000 Ωm), på djup som varierar mellan 600 och 1 500 meter. Det högresistiva berget kan endast ses ytligt i platsundersökningsområdet. I stället ses här berg med moderat resistivitet relativt nära ytan. Lågresistivt berg (500 till 1 000 Ωm) indikeras på ett djup av omkring 700 till 1 100 meter i platsundersökningsområdet.

Datakvaliteten varierade mellan stationerna. Alla stationer var påverkade av kulturellt brus, men alla utom två gav trovärdiga inversionsresultat. Felmarginalerna för lagerparametrarna är emellertid relativt stora, speciellt för lagrens resistiviteter. Det ska också påpekas att den verkliga resistivitetsfördelningen i marken knappast beskrivs av diskreta lager. En gradvis sänkning av resistiviteten med ökat djup är en mer trolig modell.

Resistivitetsvariationen med djupet tolkas bero på en ökning i salinitet. Andra faktorer, som litologi, porositet och sprickighet, förväntas inte ha någon signifikant betydelse. Däremot har två-dimensionella strukturer påverkat data. Detta är mest tydligt för en sonderingsstation i närheten av Forsmarkszonen.

Contents

1 Introduction

SKB performs site investigations for localization of a deep repository for high level radioactive waste. The site investigations are performed at two sites, Forsmark and Simpevarp/Laxemar. This document reports the results gained by Transient electromagnetic (TEM) soundings in the Forsmark area and the regional surroundings, which is one of the activities performed within the site investigation at Forsmark. The work was carried out in accordance with Activity Plan AP PF 400-06-118. In Table 1-1 controlling documents for performing this activity are listed. Both Activity Plan and Method Descriptions are SKB's internal controlling documents.

Seven TEM soundings were performed during January–February 2007. Large cable loop transmitters were used and the secondary field was measured at four to five stations for each transmitter. The position of transmitters and receiver stations can be seen in Figure 1-1. The field work was carried out by GeoVista AB and SMOY in co-operation. Processing and interpretation of data has been carried out by GeoVista AB.

The work gives input parameters to the regional geohydrological model of the Forsmark site investigation.

The results of the work are stored in the Sicada database and are traceable through the Activity Plan number AP PF 400-06-118. The locations of the seven transmitter loops are stored in Sicada according to Table 1-2.

Table 1-1. Controlling documents for the performance of the activity.

Activity Plan	**Number**	**Version**
Transient elektromagnetisk sondering i Forsmark och regional omgivning.	AP PF 400-06-118	1.0
Method Descriptions	**Number**	**Version**
Metodbeskrivning för TEM-mätning	SKB MD 212.008	1.0

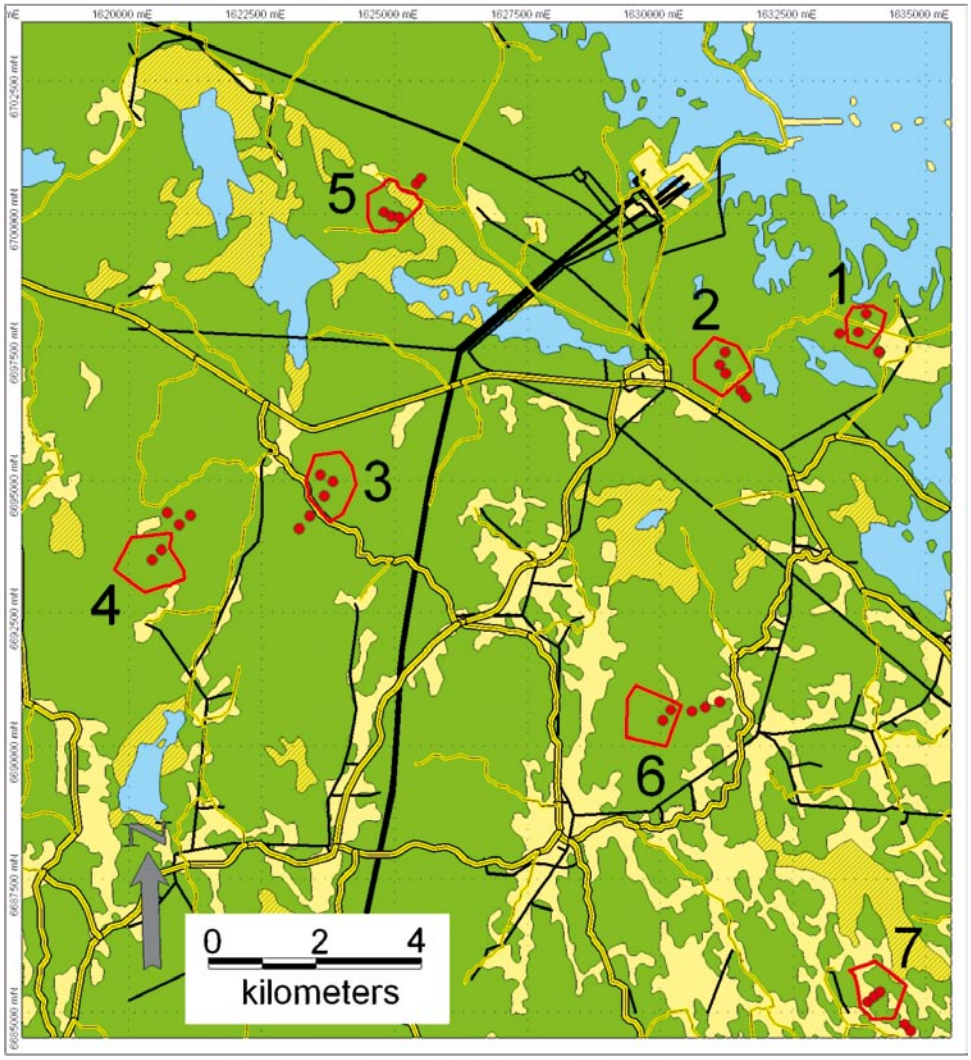

From GSD (c) Lantmäteriet Gävle 2001, Permission M2001/5268
Swedish Nuclear Fuel and Waste Management Co. 2007-07-26

Figure 1-1. *Map showing the position of cable loop transmitters (red polygons) and receiver stations (red symbols). The transmitter loops are labelled with numbers 1 to 7. The Forsmark power plant is located in the north-eastern part of the map area. Power-lines are shown in black.*

Table 1-2. Sicada Id codes of the seven transmitter loops and corresponding receiver positions.

Transmitter loop no.	Sicada Id.	Sicada Id. of receiver positions
1	AFM001332	PFM007326, PFM007327, PFM007328, PFM007329
2	AFM001333	PFM007330, PFM007331, PFM007332, PFM007333, PFM007334
3	AFM001334	PFM007335, PFM007336, PFM007337, PFM007338, PFM007339
4	AFM001335	PFM007340, PFM007341, PFM007342, PFM007343, PFM007344
5	AFM001336	PFM007345, PFM007346, PFM007347, PFM007348, PFM007349
6	AFM001337	PFM007350, PFM007351, PFM007352, PFM007353, PFM007354
7	AFM001338	PFM007355, PFM007356, PFM007357, PFM007358, PFM007359

2 Objective and scope

The presence of saline ground-water at large depth might influence the regional ground-water flow and is hence an important parameter in the assessment of the geohydrological situation in the area. The depth to and the nature of the transition to saline groundwater at depth is investigated by sampling and logging in deep boreholes in the candidate area. There are however no deep boreholes in the regional surroundings of the Forsmark area. The depth to saline water is also assumed to increase with distance from the coast-line which makes borehole investigations difficult away from the coast. The purpose of this work is to estimate the depth to rock of low electric resistivity related to saturation of pore-space with saline groundwater. Transient electromagnetic (TEM) soundings have been performed at seven locations in the Forsmark candidate area and its regional surroundings.

3 Equipment

3.1 Description of equipment and interpretation tools

The field survey was performed with a Geonics TEM-37 transmitter and a Geonics Protem receiver with a 3D receiver coil. Large cable loops were used to transmit the primary transient field. Synchronisation between the transmitter and receiver units was facilitated by oscillator crystals. The instrument was supplied by SMOY, Finland.

Orientation in the field was carried out with the help of hand-held GPS and compass. The position of transmitter loop vertices and receiver stations were determined by handheld GPS (Garmin GPSmap76S with external antenna GA 27C). The geodetic datum parameters in the GPS unit were set in accordance with the recommendations from the National Land Survey to achieve best possible compatibility with RT90.

The following software was used for processing, modelling, interpretation and visualisation of the survey data:

- EM Vision v 2.3 (Encom Technology).
- MapInfo Professional v 8.5 (MapInfo Corp.)
- Discover v 8.1 (Encom Technology).
- MathCAD 2001i Professional (Mathsoft Engineering & Education Inc.).
- Surfer v 8.0 (Golden Software).
- Grapher v 6.0 (Golden Software).

4 Execution

4.1 General

Transient Electromagnetic sounding is a geophysical method that is capable of estimating the electrical properties of the subsurface to large depths. A thorough description of the method can be found in geophysical text books, e.g. /1/, and only a brief description is given here.

A DC current is fed into a cable loop or coil, thereby producing a primary magnetic field, Figure 4-1. The current is then switched off, resulting in induced electric currents in the ground. The induced currents will diffuse downwards/outwards from the transmitter and at the same time produce a decaying secondary magnetic field. This secondary field is measured with the help of an induction coil. The magnitude and decay rate of the secondary field is a function of the resistivity distribution in the ground. Measurements at late times will give information from large depths. Multiple readings are usually stacked to improve the signal-to-noise level.

The results are usually modelled and interpreted in terms of a horizontally layered earth.

The survey was carried out in accordance with the SKB Method Description SKB MD 212.008 (SKB internal controlling document).

4.2 Preparations

Electromagnetic measurements are in general sensitive to disturbances from power lines and other cultural installations. Suitable locations for the TEM soundings were therefore identified by analysis of geographical data in a GIS. Buffer zones of 300 metres width were created around the major power lines and zones of 150 metres width were created around minor power lines. All cable loop transmitters and receiver stations were placed outside these buffer zones. Transmitter loops were also placed in such a way that some part of each of them was accessible from a road, since the transmitter generator is heavy and bulky to transport in the terrain. Whenever possible, segments of the transmitter loops were placed along e.g. small roads to make the field work easier. Coordinates for the planned loop corners and receiver stations were entered as waypoints into the GPS unit for easy location in the field. Distances and bearings between loop corners were also calculated and printed for use in the field.

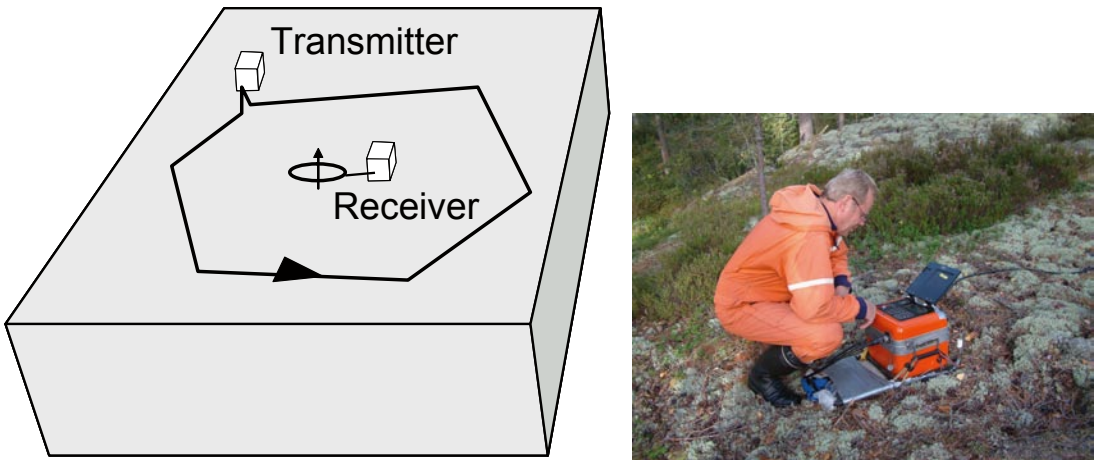

Figure 4-1. *Measurement with Transient Electromagnetic Sounding (TEM). Left, transmitter loop and receiver. Right, operator at the recording instrument close to the induction coil.*

4.3 Execution of field work

The survey was carried out with one transmitter loop at a time (Figure 1-1). The cable loop was laid out in the terrain without any previous staking. Compass, calculated bearings and GPS way-points were used for orientation.

The cable loop was connected to the transmitter unit and the output current and current turn-off ramp-time were noted. The oscillator crystals of both the transmitter and the receiver unit were warmed up and subsequently synchronized. The survey was performed with a base repetition rate of 25 Hz. This means that 50 Hz noise ideally will cancel out since every second transient is measured with opposite polarity.

The receiver antenna was placed at the survey station and levelled. The antenna was oriented in such a way that that the horizontal coils would measure in the north and east directions respectively. Measurement was performed during 15 seconds of stacking. Such a stack was then repeated 20 times at each station, giving 20 different decay curves for the measured component. All three components of the secondary field were recorded simultaneously. Measurement was performed with both high and low gain at every station. High gain might cause over-saturation in the pre-amplifier whereas low gain might reduce the sensitivity of the instrument.

The stacked decaying signal is plotted on the instrument display during measurement.
A first data quality control was therefore performed directly in the field.

The cable loop was picked up when all receiver stations had been surveyed. The whole procedure was then repeated at the next loop position.

4.4 Data handling/post processing

Raw data are stored by the instrument. Those data were downloaded to a PC at the end of each working day. An extra quality check was made and a copy of the data was then sent by E-mail to the GeoVista office in Luleå. The raw data was also handed over to SKB.

The data files were read by the program EM Vision v 2.3 and converted to the AMIRA industry standard format for TEM data. Median values, for each channel for the 20 measured decay curves, were calculated in the same process. EM Vision was also used to convert data to apparent resistivities.

The current in the transmitter loop should ideally be zero during measurement. However, a correlation between the recorded signal and the primary field magnitude can sometimes be seen, usually in the form of a ringing effect. This indicates that a weak residual current is present in the cable loop after current shut-off. A simple linear regression analysis was performed to compensate for this effect for two transmitter locations where the effect was significant.

No significant difference could be seen between measurements made with different receiver gains. All measurements were therefore treated equally.

4.5 Analyses and interpretations

The transition from fresh to saline groundwater in the Forsmark area cannot be described by a single sharp boundary. Borehole logs show both gradual increases of salinity with depth at certain depth intervals and more sudden jumps associated with water-bearing fractures. The resolution of TEM soundings is not good enough to resolve such details. Instead, the electrical structure of the ground is modelled with horizontal layers.

The results from the different receiver locations for each transmitter loop were compared. Quite similar results are expected for measurements on a layered earth. Differences might indicate presence of electrical 2D- or 3D-structures or presence of man-made objects that produce secondary fields. The horizontal components were checked for the same reason. Horizontal secondary fields will be small compared to vertical fields over a layered earth, at least close to the transmitter centre.

The vertical component data of the measured secondary field were inverted to layered earth models with the help of the program EM Vision v 2.3. Such inversion assumes that residuals are due to random, unbiased and normal distributed noise. The models were in some cases slightly adjusted by forward modelling since the noise distribution did not fulfil the above criteria.

The measurements covered two orders of magnitude in delay time. This gives a possibility to resolve a maximum of three layers in a model. Inspections of the data did however reveal different characteristics for data close to the Baltic Sea at the site investigation area, compared to data collected away from the sea. The former showed apparent resistivities in the order of 2,000 to 3,000 Ωm at early times and lower values for late times. The stations further away from the sea showed high apparent resistivities at early times (> 5,000 Ωm) and resistivities of around 2,000 to 3,000 Ωm at late times, i.e. around the same values as early-time data closer to the sea. It was therefore evident that a straightforward unconstrained inversion would result in models that did not represent the same layered sequence at all stations. Instead, a four-layer conceptual model that represents known conditions in the area was constructed /2/. The uppermost layer represents soil with low resistivity, followed by rock saturated with fresh, brackish and saline water respectively. The uppermost three layers would then be possible resolve at the sounding stations away from the sea, whereas the second layer might be too thin to be resolvable close to the sea. Since the soundings not are capable of resolving four layers it was necessary to constrain the resistivity of one or several layers in each inversion.

4.6 Nonconformities

The synchronization between transmitter and receiver relates to the time the current is switched off. The current will however not fall to zero instantaneously. Instead the current falls off as a linear ramp where the rate of decay is dependent upon the resistance and inductance in the transmitter loop. This ramp time is read from the transmitter unit display and entered into the receiver to set an appropriate delay for the receiver channels. Due to an operator error this was not done correctly for the sounding station near Storskäret (labeled 1 in Figure 1-1) in the candidate area. The receiver channels were therefore shifted towards earlier times and the first four channels actually ended up on the current ramp when there was still current flowing in the transmitter cable. Those channels could therefore not be used in the inversion. The remaining 16 channels did however produce good data and by taking the actual delay times into consideration it was still possible to invert the data for this station.

5 Results

The quality of the data varied significantly between the different sounding locations. It is not uncommon that this type of measurements is affected by cultural noise. The repeatability of the results, at least for the vertical component data, was quite good indicating low levels of random noise. However, some time gates consistently gave unusually high or low values or even reversed polarity. The same time gate was usually affected for all receiver stations for a particular transmitter loop. These obviously erroneous readings were however repeatable, so stacking and averaging could not be used to reduce the effect of the problem. Different time gates were affected for different transmitter loops. It seems like this problem is caused by some coherent noise, probably related to the power-line frequency 50 Hz. The data were modelled and interpreted by disregarding the obviously erroneous channels.

Strong secondary fields due to fences were recorded for the sounding station at Lundsvedja (labelled 7 in Figure 1-1). Obviously these fences formed closed loops. The secondary fields due to the fences masked the response from the ground to such an extent that it was not possible to invert the data into a layered model for this transmitter loop.

Horizontal component data are more affected by magnetotelluric fields than vertical component data, and therefore have lower signal-to-noise ratios compared to the vertical component.

The data were modelled with one-dimensional, horizontally layered models. For this type of model to be valid, it is important to verify that effects from two- or threedimensional electrical structures can be neglected. Considering the large depth of investigation, the vertical component data should be practically independent of receiver location for a one-dimensional earth. The magnitude of the horizontal components should also be considerably smaller than the vertical component for a one-dimensional earth. These criteria were reasonably well fulfilled for three of the stations. One station was affected by what was interpreted as a 2D structure. The data was still inverted to a one-dimensional model, but the results of that inversion should be treated with great care.

The results for each transmitter loop are presented below.

5.1 Transmitter loop 1

Transmitter loop 1 was located within the candidate area, not far from Storskäret (Figure 1-1). The receiver channels were by mistake offset by around 0.15 ms towards earlier times for this station (see section 4.6). Measurements were made at four stations, of which two were located outside the transmitter loop. The direction of the secondary field was analyzed to investigate the validity of a one-dimensional earth in the interpretation. The secondary field is close to vertical for the stations inside the loop (Figure 5-1) and also quite steep outside the loop. The horizontal component is larger outside the loop compared to inside and points almost radially outwards from the loop centre (Figure 5-1). All this is consistent with a one-dimensional earth and a horizontally stratified inversion model is therefore justified.

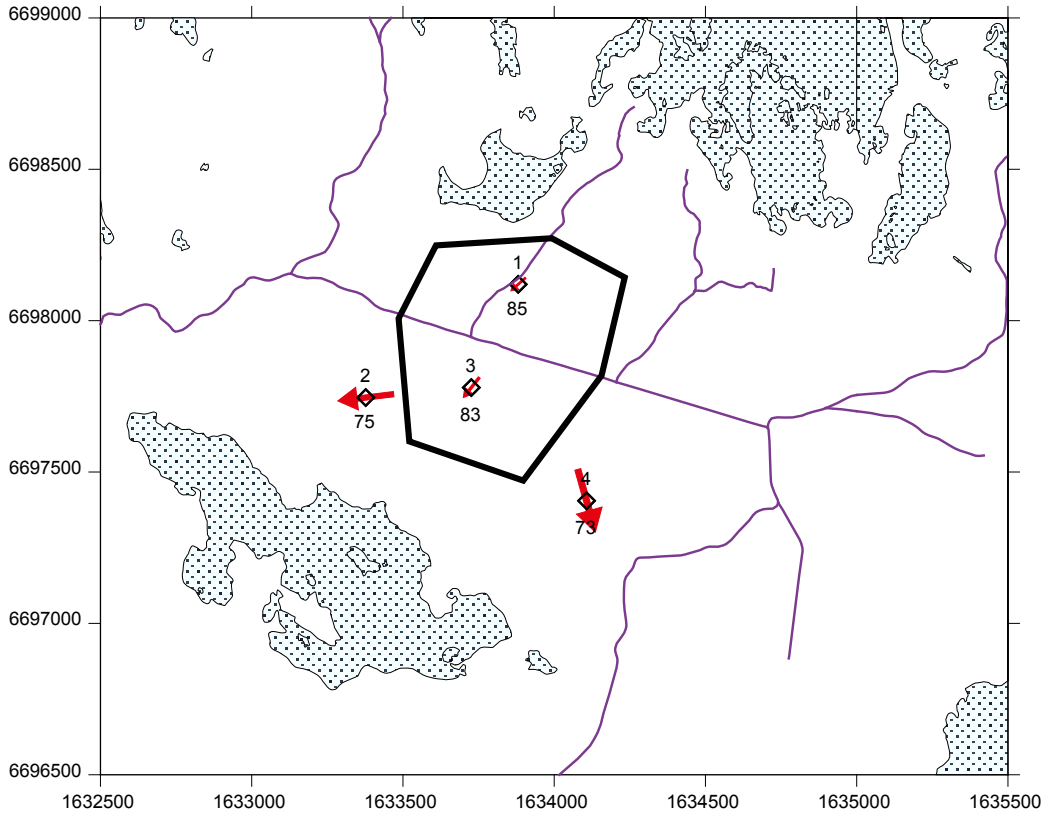

Figure 5-1. *Map showing the positions of transmitter loop 1 (thick black line) and the receiver stations used for that loop (black symbols). The station IDs are shown as labels over the symbols. The labels under the symbols indicate the inclination in degrees of the secondary field from the horizontal plane for channel 7 (0.204 ms delay time). The red arrows indicate the direction and magnitude of the horizontal secondary field for channel 7.*

The decay of the vertical component of the secondary field, seen in Figure 5-2, is quite similar for all four stations. The earliest channel shown in the figure, and to some extent the second, shows a different character for stations inside the loop compared to outside the loop. This is interpreted as being due to a residual current flowing in the transmitter cable during these channels. Those channels have therefore not been used in the inversion. The decay rate of the vertical component is slightly slower than the decay for a homogeneous half-space, indicating a decrease of resistivity with depth. The magnitude of the secondary field for channels around 0.5 ms corresponds to the response of a half space of around 2,000 to 2,500 Ωm. The corresponding half-space for late channels would have a resistivity of around 1,500 Ωm. This means that although a decrease of resistivity with depth seems significant, it is probably of low resistivity contrast. A close look at the data shows that there is an east-west trend in the magnitude of the data with larger magnitudes towards west. This would be indicative of a more low-resistivity environment towards west.

The secondary field data for transmitter loop 1 were inverted for each station separately. The start model consisted of four layers. The number of layers was chosen from a conceptual model of the geology of the area /2/. The uppermost layer corresponds to the soil cover and the parameters for that layer were free during inversion. The second layer corresponds to bedrock saturated with fresh water. The resistivity of this layer was held fixed at 10,000 Ωm during the inversion. This layer must be quite thin to be compatible with the data and would be transparent to the TEM sounding. However, the layer was included to get continuity with the models further inland and also because near-surface high-resistivity rock is known to exist from DC resistivity measurements in the area /3/. The two upper layers are quite poorly constrained by the TEM data and the inversion results for those layers should not be regarded as accurate. The third layer consists of bedrock saturated with brackish water. The resistivity of that layer was held constant at 3,500 Ωm during the inversion. The choice of resistivity was taken from the apparent resistiv-

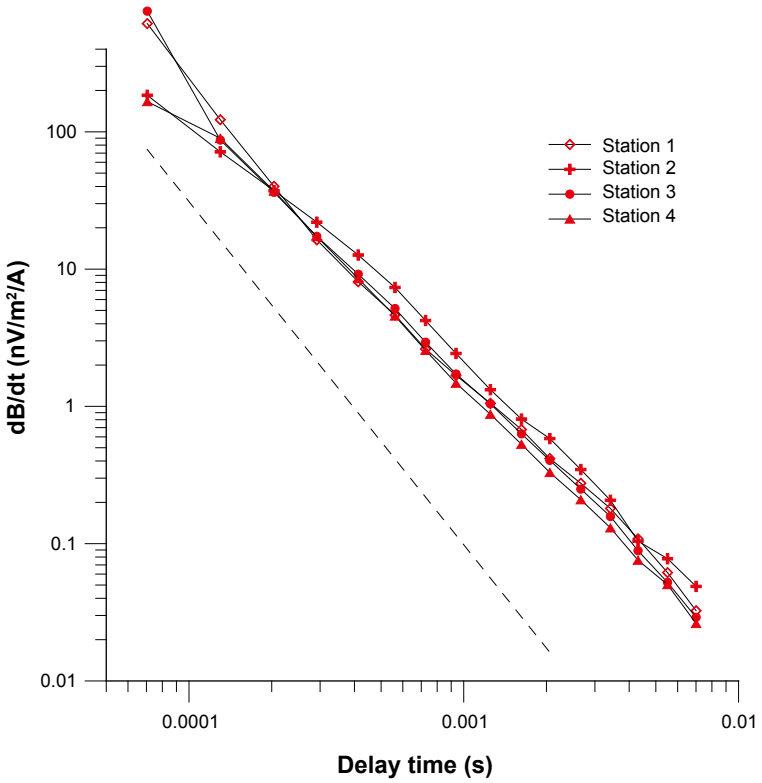

Figure 5-2. *Secondary field decay curves, vertical component, transmitter loop 1. The positions of the stations can be seen in Figure 5-1. The dashed line corresponds to decay proportional to $t^{-2.5}$, indicative of late-time homogeneous half-space response for the vertical component.*

ity values of the sounding, compensating for a bias due to the effect of the overburden. The substratum of the model consists of bedrock saturated with saline water. The resistivity of this layer was set to 1,000 Ωm and held constant, since the data indicates a low resistivity contrast. The value is compatible with resistivity measurements on drill-cores from the area saturated in saline water (e.g. /4, 5, 6, 7/).

The inversion results differed slightly for data from the four receiver stations. The uppermost layer got a resistivity of around 80 Ωm and a thickness of around 18 metres at all stations. The thickness is probably overestimated compared to what is known from e.g. DC resistivity soundings /3/. The second high-resistivity layer got thicknesses of around 100 metres in all models. This is a poorly constrained value but it is however clear that high-resistivity rock cannot extend to much larger depths in this area. The thickness of the third layer varied from 615 m (station 2) to 1,135 m (station 4). There is an east-west trend in the inversion results with increasing depth to the substratum towards east. It should however be noted that the small resistivity contrast between the layers results in fairly large error bounds for the thickness of layer three. The fit between field data and model response for station 4 can be seen in Figure 5-3. The fit is good except for the early channels where a good fit to a one-dimensional model is not possible. Equally good fits were achieved for the other stations.

The inversions were based on the vertical component of the secondary field. However, forward solutions for the inversion output models can be calculated for the horizontal components. The calculated east and north components of the secondary field can be compared with field data for station 4 in Figure 5-4. The noise threshold is at around 0.1 nV/m^2/A for the horizontal components, so the late channels should be disregarded. There is a good agreement for the north component except for the first two channels. The measured east component is however of weaker magnitude than the corresponding model response. Since this is the smaller of the two component the misfit will however be explained by a slight clock-wise rotation of the horizontal secondary field. The rocks in this area are known to have an EW to WNW-ESE azimuthal electric anisotropy /3/ that might be responsible for such a rotation.

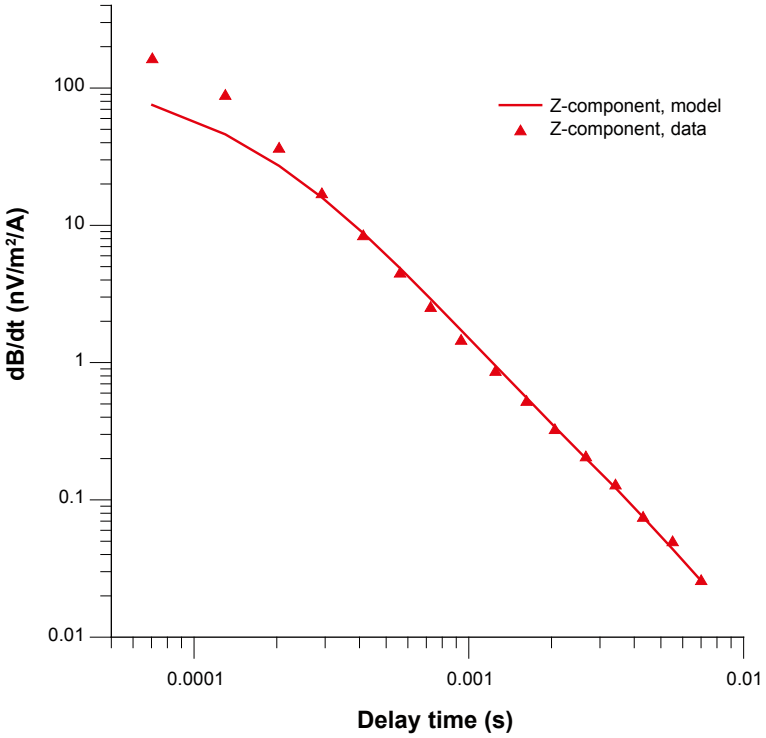

Figure 5-3. *Secondary field, vertical component, transmitter loop 1, station 4.*

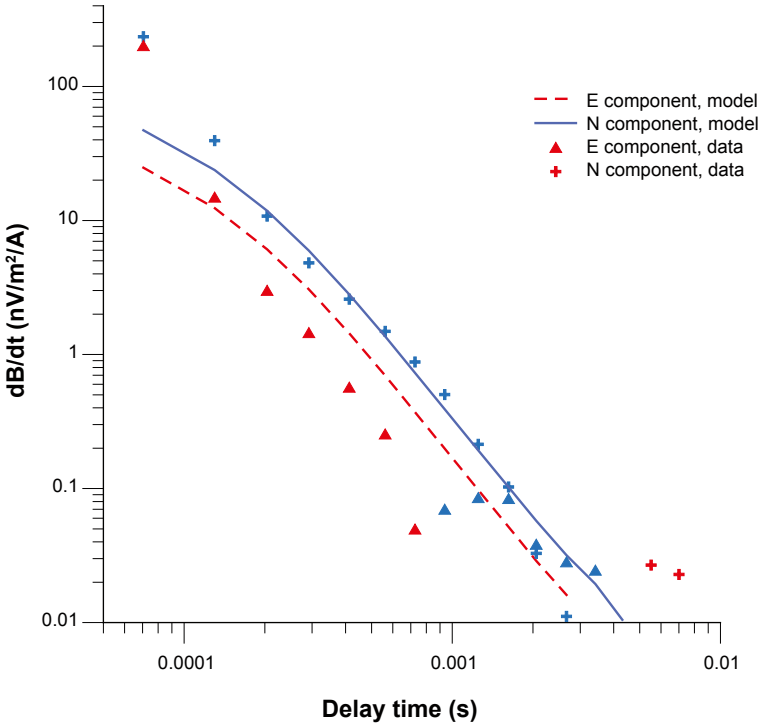

Figure 5-4. *Secondary field, horizontal components, transmitter loop 1, station 4. Red curves/symbols correspond to positive data whereas blue curves/symbols correspond to negative data.*

5.2 Transmitter loop 2

Transmitter loop 2 was located south of the candidate area, west of the lake Eckarfjärden (Figure 1-1). Measurements were made at five stations, of which two were located outside the transmitter loop. The direction of the secondary field was analyzed to investigate the validity of a one-dimensional earth in the interpretation. The secondary field is tilting towards east for all stations (Figure 5-5). This might indicate a roughly NS trending 2D structure to the west of the centre of the loop. If the decay rate of the secondary field is studied it can however be seen that the decay rate of the vertical components (Figure 5-6) is more or less the same as the decay rate of the east component (Figure 5-7), i.e. the tilt of the secondary field is roughly constant through the whole transient decay for all stations. This seems quite unlikely for a 2D structure. Instead it is suggested that the interface to conductive rock at depth is dipping towards east with as much as around 10° to 15° in this area. Inversion results based on a one-dimensional model should therefore be treated with some care but inversion would still be justified.

The decay of the vertical component of the secondary field, seen in Figure 5-6, is quite similar for all five stations, except for some channels in the time range 0.85 to 3.7 ms. Some of the channels in this time interval show data with unusually low values, sometimes negative, and some channels have unusually high values. This effect was repeatable and could not be corrected by repeated measurements and averaging. The reason to the problem is most likely some interference from 50 Hz noise. The channels in the above time interval were not included in the inversion. The earliest channel shown in the figure shows a different character for stations inside the loop compared to outside the loop. This is interpreted as being due to a residual current flowing in the transmitter cable during this channel and it was therefore not used in the inversion.

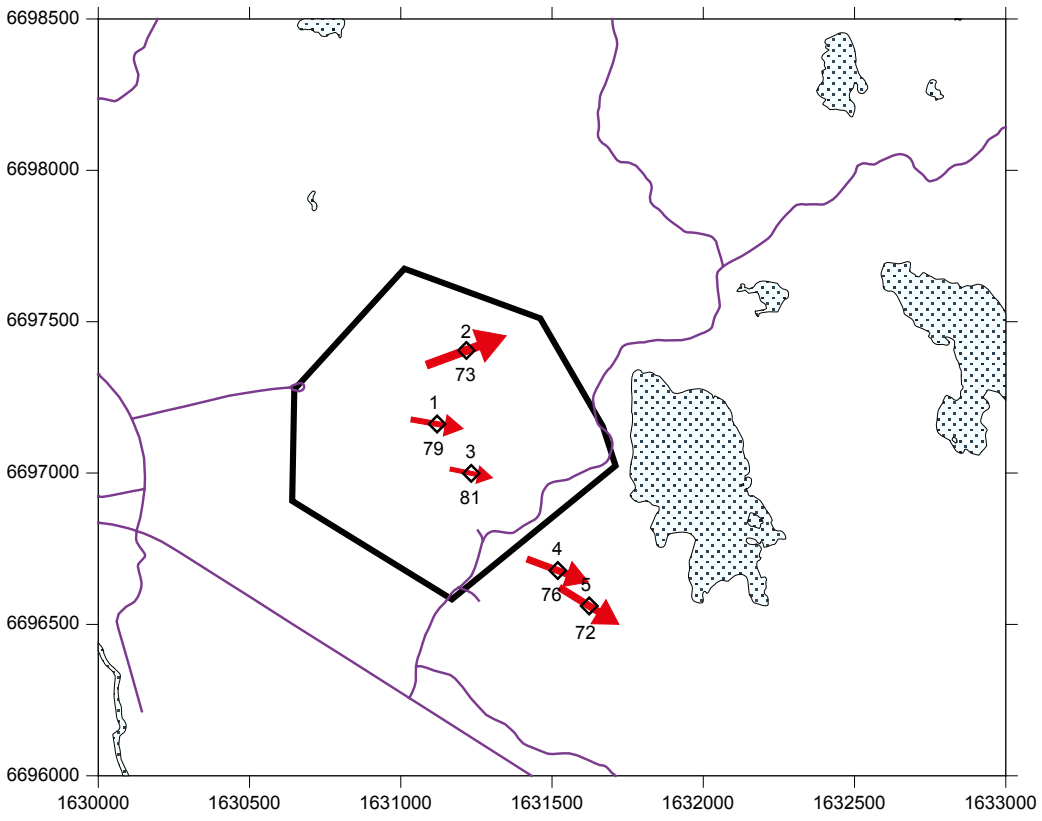

Figure 5-5. *Map showing the positions of transmitter loop 2 (thick black line) and the receiver stations used for that loop (black symbols). The station IDs are shown as labels over the symbols. The labels under the symbols indicate the inclination in degrees of the secondary field from the horizontal plane for channel 4 (0.176 ms delay time). The red arrows indicate the direction and magnitude of the horizontal secondary field for channel 4.*

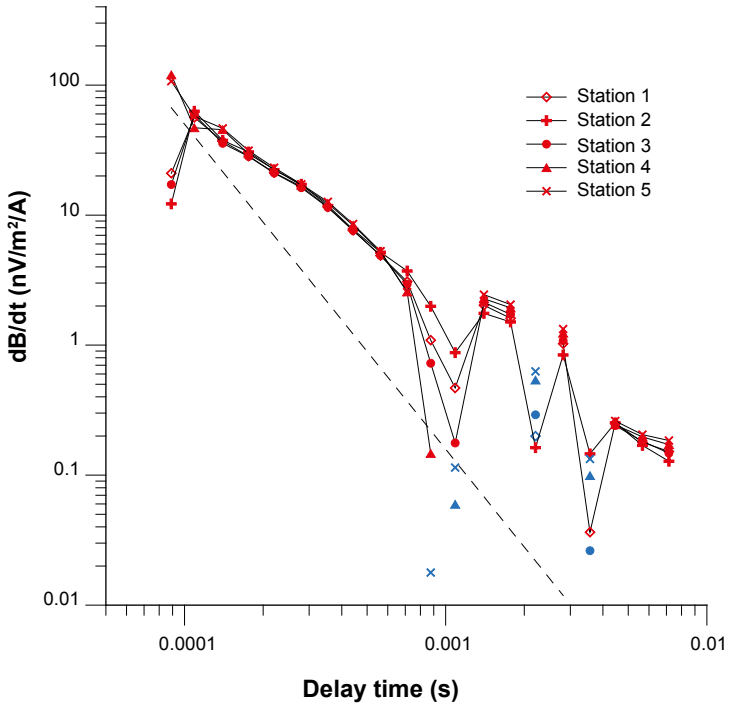

Figure 5-6. *Secondary field decay curves, vertical component, transmitter loop 2. The positions of the stations can be seen in Figure 5-5. The dashed line corresponds to decay proportional to $t^{-2.5}$, indicative of late-time homogeneous half-space response for the vertical component. Red symbols correspond to positive data whereas blue symbols correspond to negative data.*

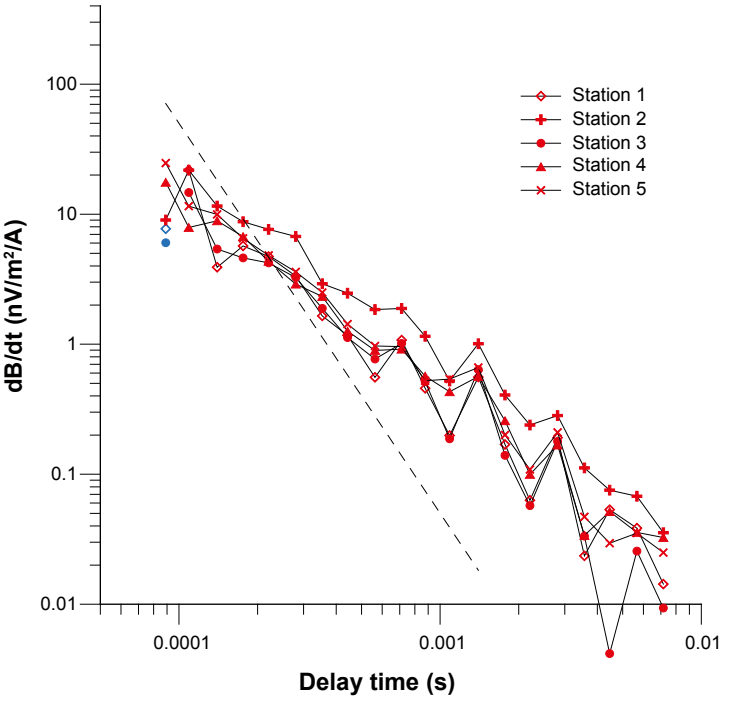

Figure 5-7. *Secondary field decay curves, east component, transmitter loop 2. The positions of the stations can be seen in Figure 5-5. The dashed line corresponds to decay proportional to t^{-3}, indicative of late-time homogeneous half-space response for horizontal components. Red symbols correspond to positive data whereas blue symbols correspond to negative data.*

The decay rate of the vertical component is clearly slower than the decay for a homogeneous half-space, indicating a decrease of resistivity with depth. The magnitude of the secondary field for early channels corresponds to the response of a half space of around 4,000 Ωm. The corresponding half-space for late channels would have a resistivity of around 900 Ωm.

The inversion results were similar for all receiver stations. The same type of four-layer model as the one used for transmitter loop 1 was used (see section 5.1). A tilt towards east of the interface to a conducting substratum would possibly result in larger depths during inversion of stations to the east. The reason that no such effect can be seen might be that the stations are located more or less along a NS profile. The uppermost layer got a resistivity of around 450 Ωm and a thickness of around 8 metres in the inversion. This layer is however more or less transparent to the sounding. The inversion output for the second high-resistivity layer was a thickness of 265 metres and a resistivity of 12,400 Ωm, whereas the values for the third layer were 2,500 Ωm and 575 metres. The resistivity of the third layer was held fixed during the inversion. The resistivity of the substratum was held fixed at 500 Ωm during the inversion. The fit between field data and model response for station 4 can be seen in Figure 5-8. The fit is good except for the noisy channels mentioned above. That noise and the deviation from a true one-dimensional earth should however be kept in mind when the output of the inversion is assessed. The general features of the inversion model are however reasonable and can be regarded as quite reliable, although the actual numeric values might be inaccurate.

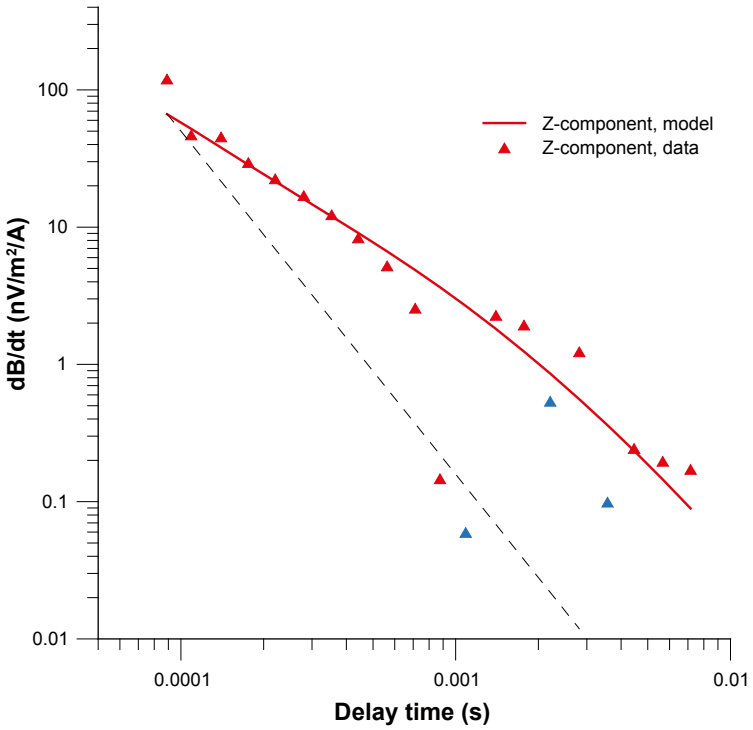

Figure 5-8. *Secondary field, vertical component, transmitter loop 2, station 4. The dashed line corresponds to decay proportional to $t^{-2.5}$, indicative of late-time homogeneous half-space response for the vertical component. Red symbols correspond to positive data whereas blue symbols correspond to negative data.*

5.3 Transmitter loop 3

Transmitter loop 3 was located near Berkinge, around 8 km south-west of Forsmark power plant (Figure 1-1). Measurements were made at five stations, of which two were located outside the transmitter loop. The direction of the secondary field was analyzed to investigate the validity of a one-dimensional earth in the interpretation. The secondary field is fairly steep for the stations inside the loop (Figure 5-9) and also quite steep outside the loop. The horizontal component is larger outside the loop compared to inside and points almost radially outwards from a point slightly west of the loop centre (Figure 5-9). All this is consistent with a one-dimensional earth and a horizontally stratified inversion model is therefore justified.

The decay of the vertical component of the secondary field, seen in Figure 5-10, is quite similar for all five stations. The decay rate of the vertical component is somewhat slower than the decay for a homogeneous half-space, indicating a decrease of resistivity with depth. The magnitude of the secondary field for early channels corresponds to the response of a half space of around 7,500 Ωm. The corresponding half-space for late channels would have a resistivity of around 3,500 Ωm.

The inversion results were similar for all receiver stations. The same type of four-layer model as the one used for transmitter loop 1 was used (see section 5.1). The uppermost layer got a resistivity of around 100 Ωm and a thickness of around 12 metres in the inversion. This layer is however not well resolved by the sounding. The inversion output for the second high-resistivity layer was a thickness of 700 metres and a resistivity of 19,700 Ωm, whereas the values for the

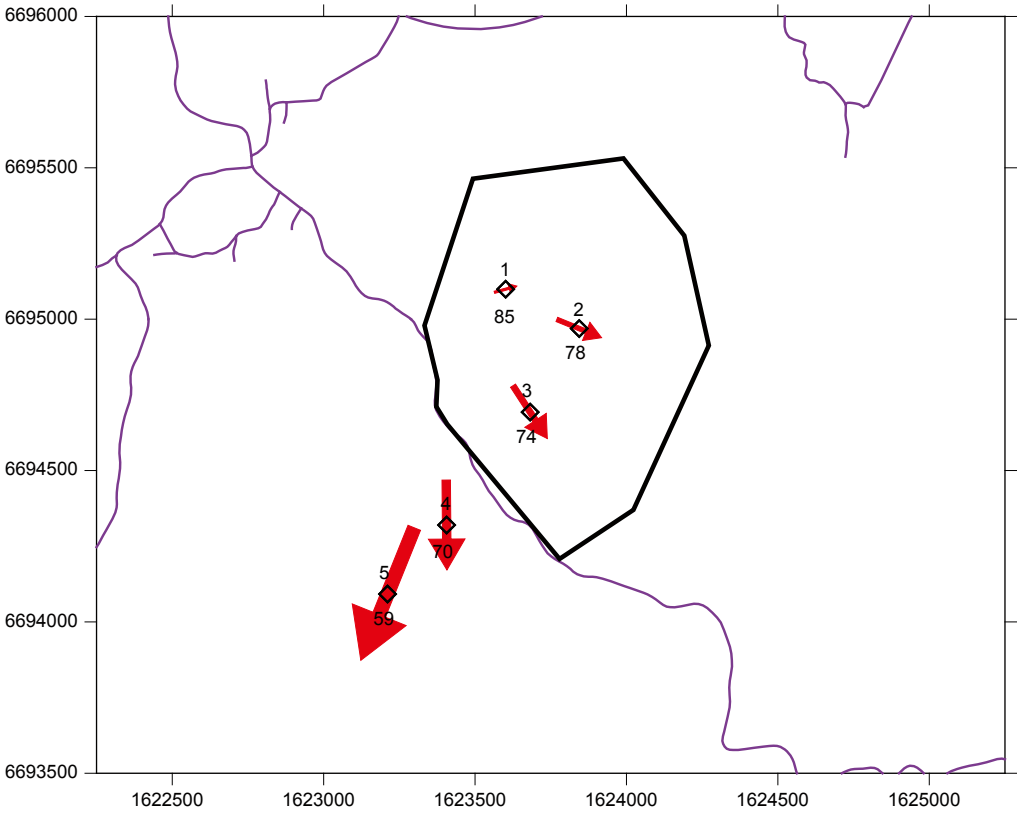

Figure 5-9. *Map showing the positions of transmitter loop 3 (thick black line) and the receiver stations used for that loop (black symbols). The station IDs are shown as labels over the symbols. The labels under the symbols indicate the inclination in degrees of the secondary field from the horizontal plane for channel 4 (0.176 ms delay time). The red arrows indicate the direction and magnitude of the horizontal secondary field for channel 4.*

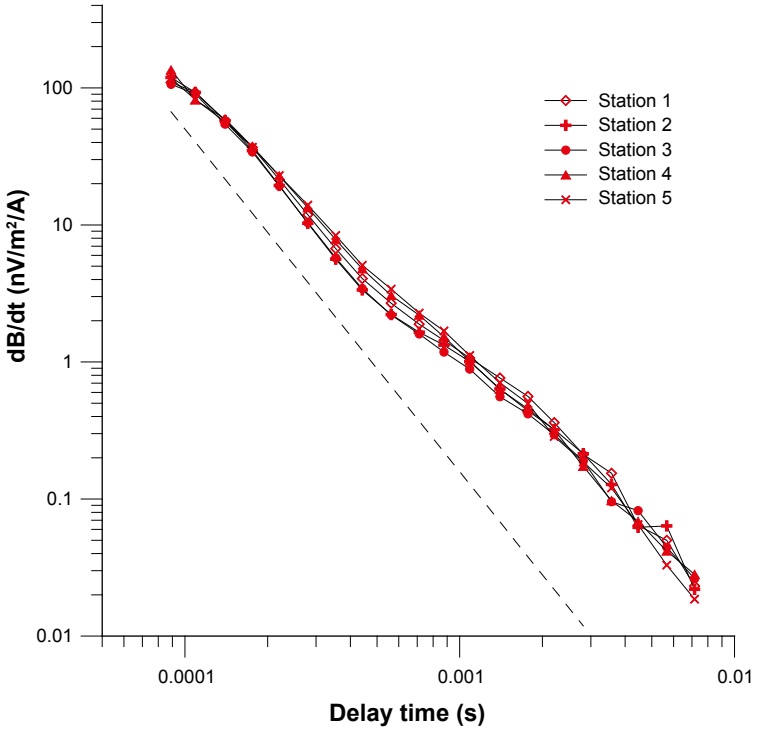

Figure 5-10. *Secondary field decay curves, vertical component, transmitter loop 3. The positions of the stations can be seen in Figure 5-9. The dashed line corresponds to decay proportional to $t^{-2.5}$, indicative of late-time homogeneous half-space response for the vertical component.*

third layer were 3,500 Ωm and 1,080 metres. The resistivity of the third layer was held fixed during the inversion. The resistivity of the substratum was held fixed at 1,000 Ωm during the inversion. The fit between field data and model response for station 5 can be seen in Figure 5-11. The fit is reasonably good except for the first two channels that cannot be fitted to a layered model.

The inversions were based on the vertical component of the secondary field. However, forward solutions for the inversion output models can be calculated for the horizontal components. The calculated east and north components of the secondary field can be compared with field data for station 5 in Figure 5-12. The noise threshold is at around 0.1 nV/m^2/A for the horizontal components, so the late channels should be disregarded. The agreement between field data and model response is quite good for the north component. The measured east component is however of weaker magnitude than the corresponding model response. The misfit corresponds to a counterclock-wise rotation of the horizontal secondary field. Also the total magnitude of the measured horizontal field is smaller than the model response. The layered model still seems plausible when the horizontal field is considered.

5.4 Transmitter loop 4

Transmitter loop 4 was located near Håkansbo, around 12 km south-west of Forsmark power plant (Figure 1-1). Measurements were made at five stations, of which three were located outside the transmitter loop. The direction of the secondary field was analyzed to investigate the validity of a one-dimensional earth in the interpretation. The secondary field is fairly steep for the stations inside the loop (Figure 5-13) and also quite steep outside the loop. The horizontal component is larger outside the loop compared to inside and, except for station 1, points away from the loop centre (Figure 5-13). All this is consistent with a one-dimensional earth and a horizontally stratified inversion model is therefore justified.

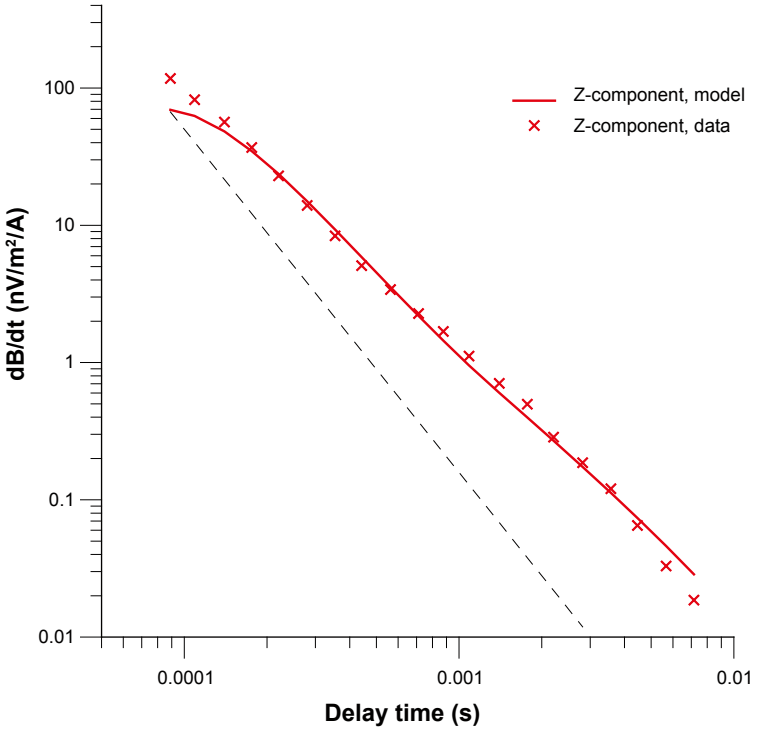

Figure 5-11. *Secondary field, vertical component, transmitter loop 3, station 5. The dashed line corresponds to decay proportional to $t^{-2.5}$, indicative of late-time homogeneous half-space response for the vertical component.*

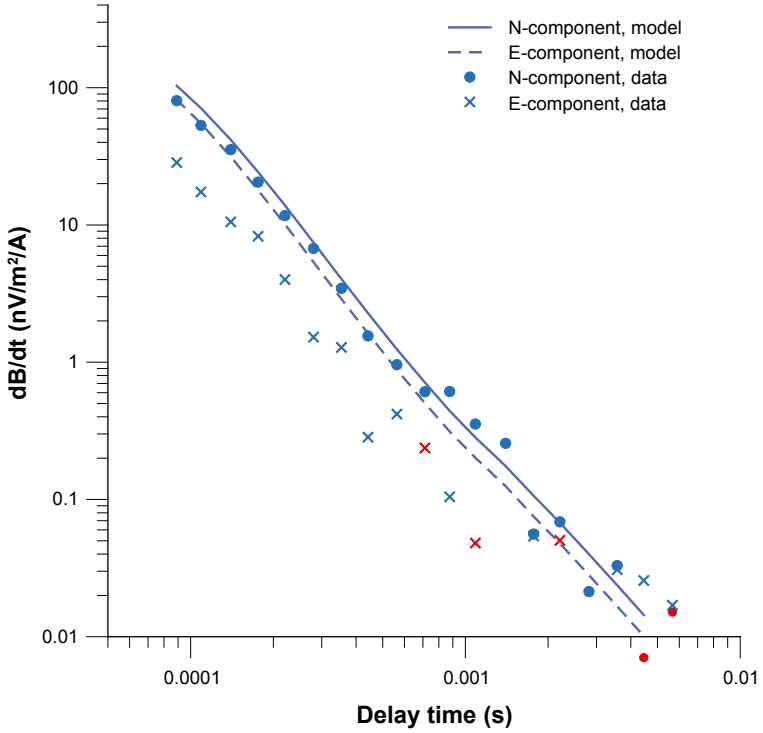

Figure 5-12. *Secondary field, horizontal components, transmitter loop 3, station 5. Red curves/symbols correspond to positive data whereas blue curves/symbols correspond to negative data.*

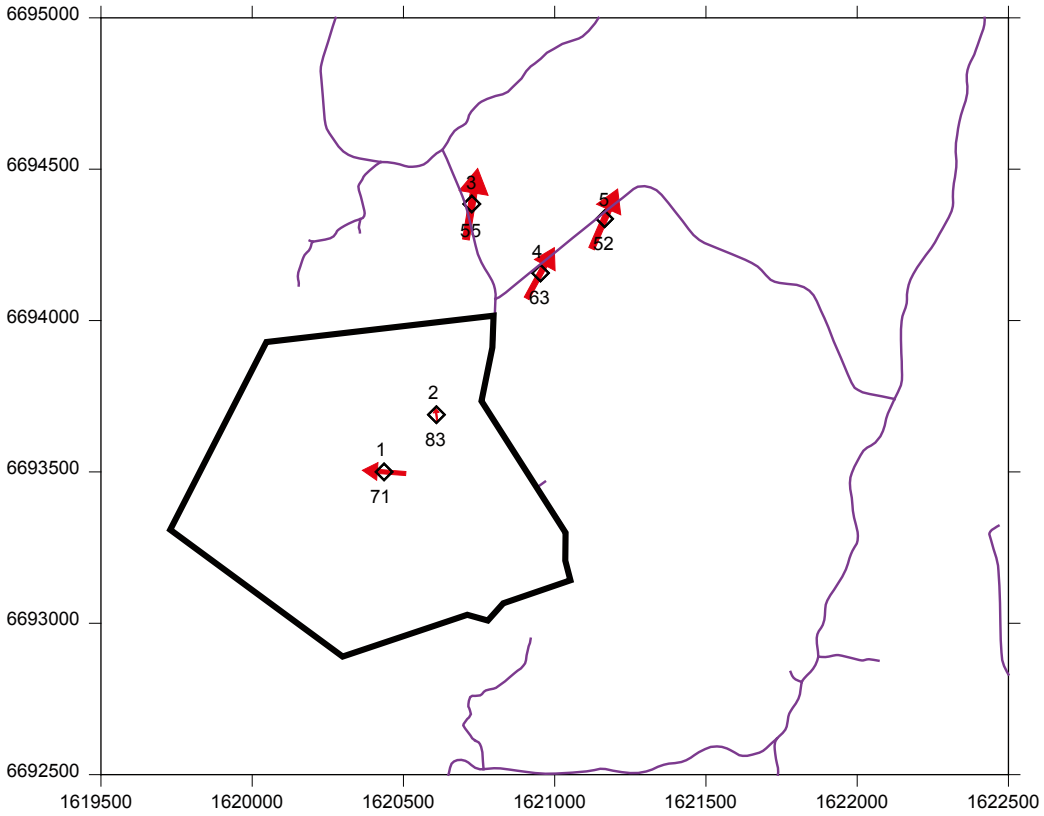

Figure 5-13. *Map showing the positions of transmitter loop 4 (thick black line) and the receiver stations used for that loop (black symbols). The station IDs are shown as labels over the symbols. The labels under the symbols indicate the inclination in degrees of the secondary field from the horizontal plane for channel 4 (0.176 ms delay time). The vertical component data used to calculate the direction has been corrected for an assumed residual current in the transmitter loop. The red arrows indicate the direction and magnitude of the horizontal secondary field for channel 4.*

The decay of the vertical component of the secondary field, seen in Figure 5-14, differs between the stations. The stations inside the loop have stronger signals at early channels and weaker signals at intermediate channels compared to stations outside the loop. It is difficult to imagine any true resistivity distribution in the ground that would result in such a secondary field. Instead this is interpreted as a "loop effect", i.e. a field due to a residual current flowing in the transmitter loop. The magnitude of this current was estimated by assuming a measured signal:

$S_z = F_z + C \cdot dI/dt$

Where S_z is the measured signal, F_z is the true secondary field from the ground, C is the loop-receiver coupling and dI/dt is the time derivative of the current in the loop. F_z will be more or less the same for all receiver stations if the effect of 2D and 3D structures can be neglected. C is a purely geometric factor that can be calculated and it is also measured by the instrument during the current turn-off ramp. This means that a plot of S_z versus C would result in a straight line for a certain channel. The slope of the line would correspond to dI/dt. The "loop effect" was estimated in the above way and subtracted from the measured data. This resulted in corrected vertical component data shown in Figure 5-15. The decay curves now look quite similar except for the earliest channels. The data in Figure 5-15 were used for inversion.

The decay rate of the corrected vertical component in Figure 5-15 is somewhat slower than the decay for a homogeneous half-space, indicating a decrease of resistivity with depth. The magnitude of the secondary field for early channels corresponds to the response of a half space of around 7,500 Ωm to 10,000 Ωm. The corresponding half-space for late channels would have a resistivity of around 5,000 to 6,000 Ωm.

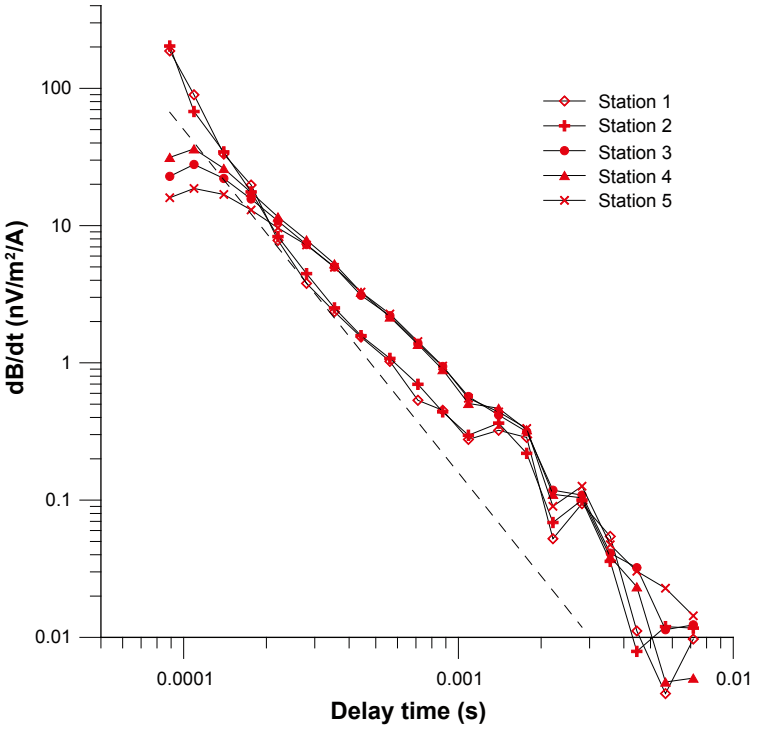

Figure 5-14. *Secondary field decay curves, vertical component, transmitter loop 4. The positions of the stations can be seen in Figure 5-13. The dashed line corresponds to decay proportional to $t^{-2.5}$, indicative of late-time homogeneous half-space response for the vertical component.*

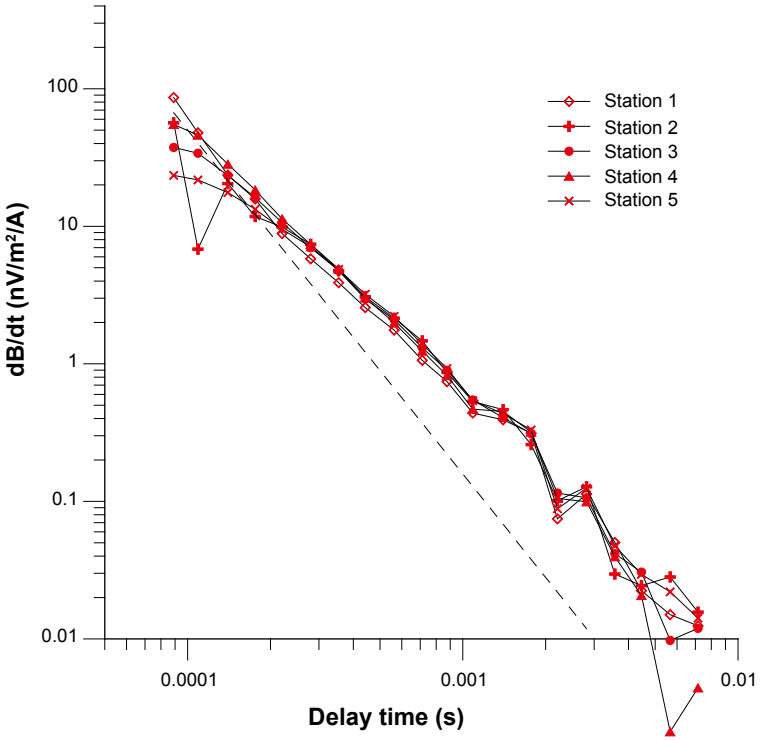

Figure 5-15. *Secondary field decay curves, vertical component, transmitter loop 4, corrected for the "loop effect". The positions of the stations can be seen in Figure 5-13. The dashed line corresponds to decay proportional to $t^{-2.5}$, indicative of late-time homogeneous half-space response for the vertical component.*

The inversion results were similar for all receiver stations. The same type of four-layer model as the one used for transmitter loop 1 was used (see section 5.1). The uppermost layer got a resistivity of around 390 Ωm and a thickness of around 25 metres in the inversion. This layer is however not well resolved by the sounding. The inversion output for the second high-resistivity layer was a thickness of 1,500 metres and a resistivity of 16,250 Ωm, whereas the values for the third layer were 3,500 Ωm and 5,000 metres. The resistivity of the third layer was held fixed during the inversion. The resistivity of the substratum was held fixed at 500 Ωm during the inversion. The thickness of the third layer is so large that the substratum does not affect the model response. This turns the model effectively into a three-layer model and the low-resistivity fourth layer is not detected by the sounding. There is no unique way to estimate a minimum depth to a possible low-resistivity substratum without assuming certain parameters for the other layers. No layer with a resistivity in the range 500 to 1,000 Ωm can however exist at a depth of less than around 2,500 m. The fit between field data and model response for station 4 can be seen in Figure 5-16. The fit is good except for the last two channels that are below the noise threshold.

The inversions were based on the vertical component of the secondary field. However, forward solutions for the inversion output models can be calculated for the horizontal components. The calculated east and north components of the secondary field can be compared with field data for station 4 in Figure 5-17. The noise threshold is at around 0.1 nV/m²/A for the horizontal components, so the intermediate and late channels should be disregarded. The agreement between field data and model response is reasonably good. The layered model thus seems plausible when the horizontal field is considered.

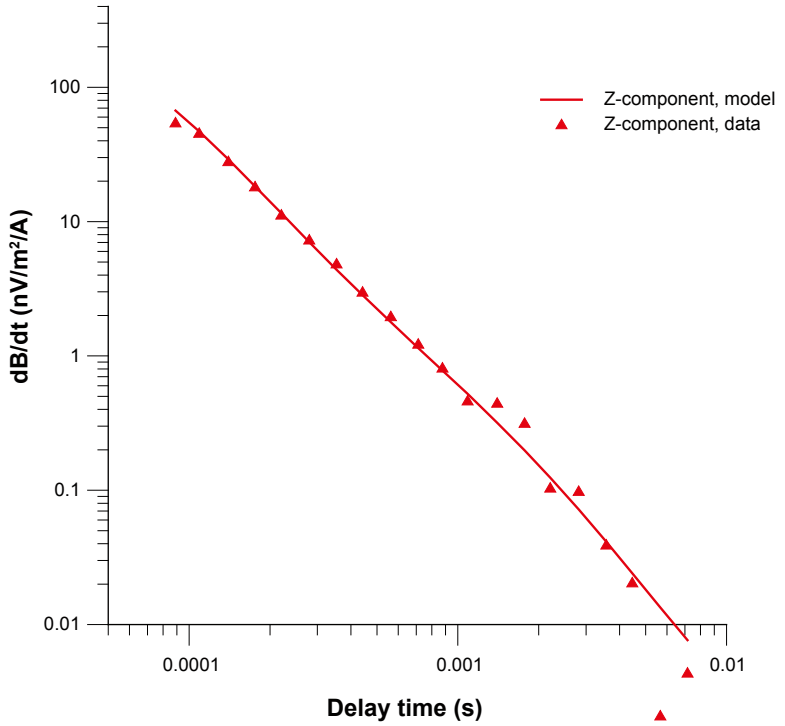

Figure 5-16. *Secondary field, vertical component, transmitter loop 4, station 4. The data have been corrected for the "loop effect".*

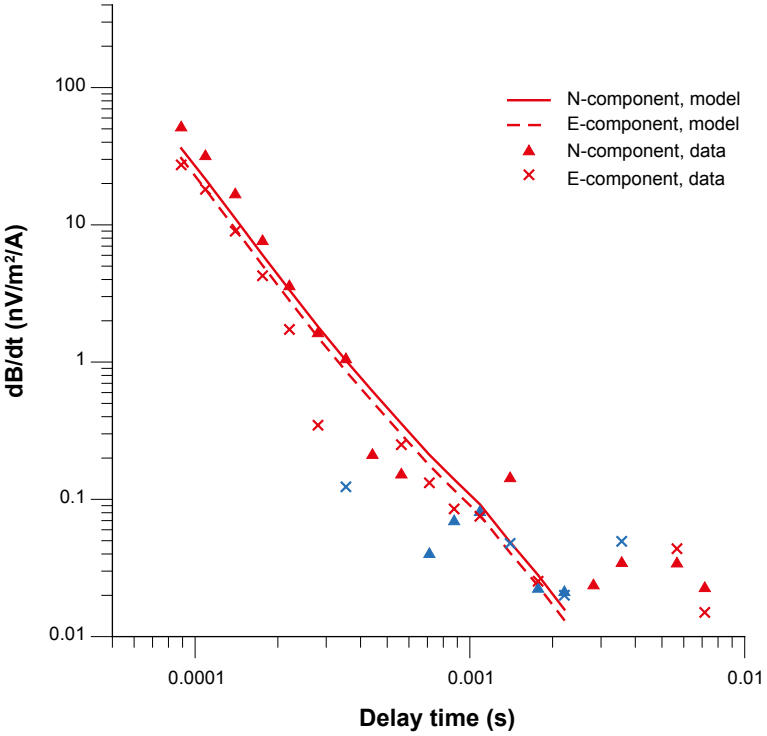

Figure 5-17. *Secondary field, horizontal components, transmitter loop 4, station 4. Red curves/symbols correspond to positive data whereas blue curves/symbols correspond to negative data.*

5.5 Transmitter loop 5

Transmitter loop 5 was located near Björnbo, around 5 km west of Forsmark power plant (Figure 1-1). Measurements were made at five stations, of which two were located outside the transmitter loop. The direction of the secondary field was analyzed to investigate the validity of a one-dimensional earth in the interpretation. The secondary field is fairly steep for the stations inside the loop (Figure 5-18) but makes an angle to the horizontal plane of less than 40° outside the loop. The horizontal component points in a north-east direction with a similar magnitude for all stations. This indicates a 2D structure in a NW-SE direction that is electrically conductive. A layered-earth model is therefore hardly valid. Inversion has still been carried out, but the results should be treated with great care.

The decay of the vertical component of the secondary field, seen in Figure 5-19, differs between the stations. The stations inside the loop have stronger signals at early channels and weaker signals at late channels compared to stations outside the loop. It is difficult to imagine any true resistivity distribution in the ground that would result in such a secondary field. Instead this is interpreted as a "loop effect", i.e. a field due to a residual current flowing in the transmitter loop. The magnitude of this current was estimated and corrected for in the same way as for loop 4 (see section 5.4). This resulted in corrected vertical component data shown in Figure 5-20. The decay curves now look quite similar except for the earliest channels. The correction method builds upon the assumption that the vertical component is more or less independent on position. This is true for a layered earth but not necessarily when 2D-structures are present, as in this area. The corrected data in Figure 5-20 do however seem reasonable.

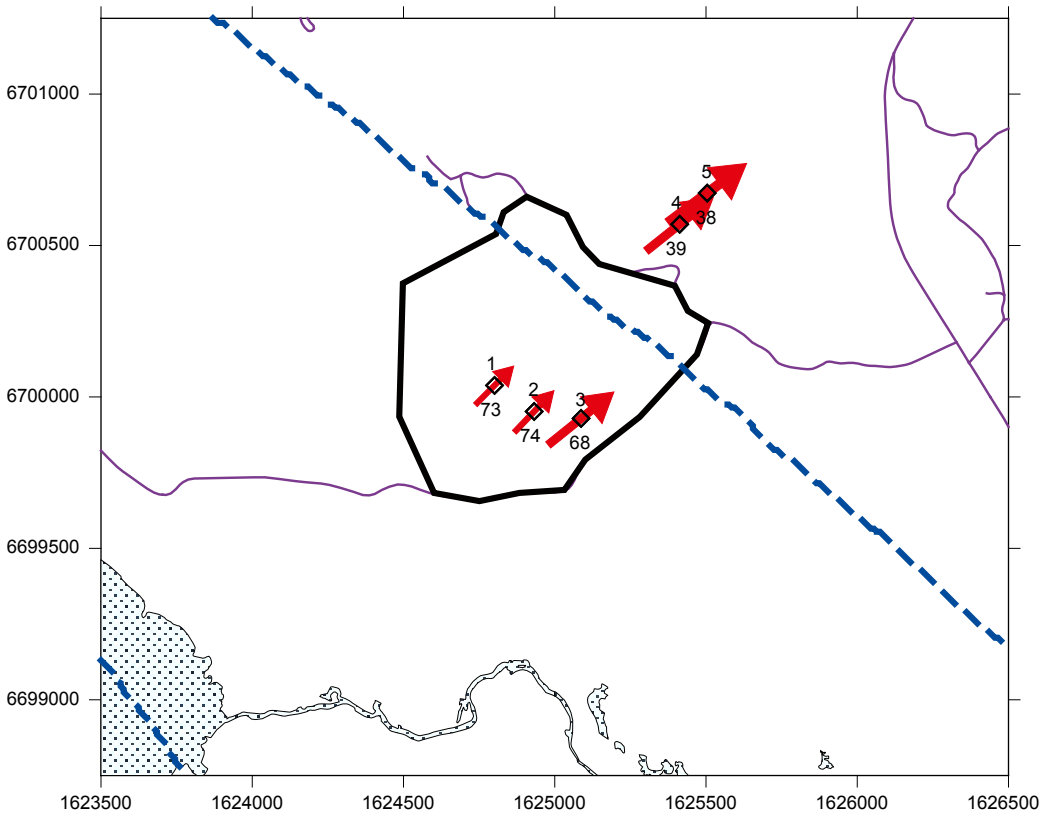

Figure 5-18. *Map showing the positions of transmitter loop 5 (thick black line) and the receiver stations used for that loop (black symbols). The station IDs are shown as labels over the symbols. The labels under the symbols indicate the direction in degrees of the secondary field from the horizontal plane for channel 4 (0.176 ms delay time). The vertical component data used to calculate the direction has been corrected for an assumed residual current in the transmitter loop. The red arrows indicate the inclination and magnitude of the horizontal secondary field for channel 4. Deformation zones are shown with dashed blue lines.*

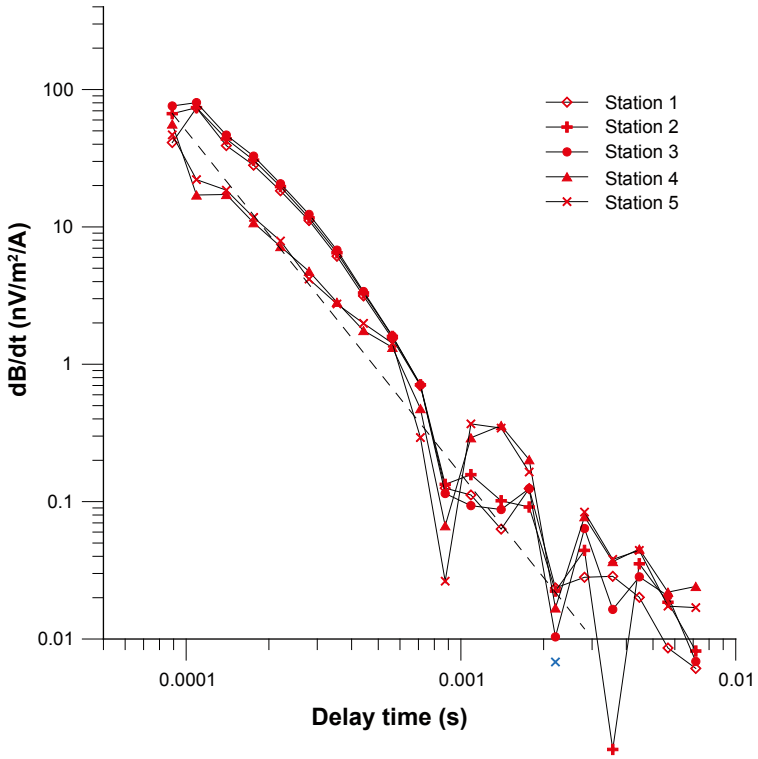

Figure 5-19. *Secondary field decay curves, vertical component, transmitter loop 5. The positions of the stations can be seen in Figure 5-18. The dashed line corresponds to decay proportional to $t^{-2.5}$, indicative of late-time homogeneous half-space response for the vertical component. Red symbols correspond to positive data whereas blue symbols correspond to negative data.*

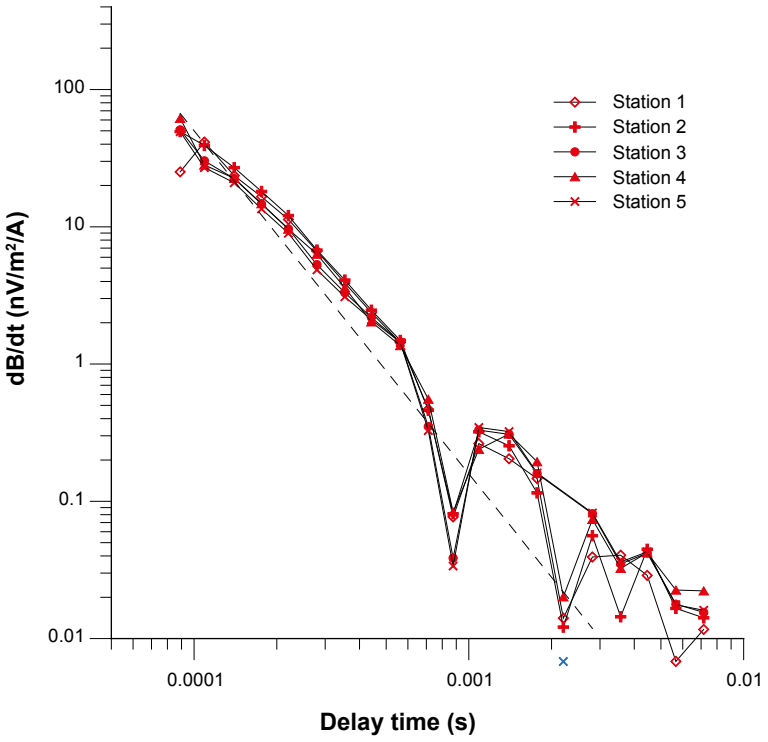

Figure 5-20. *Secondary field decay curves, vertical component, transmitter loop 5, corrected for the "loop effect". The positions of the stations can be seen in Figure 5-18. The dashed line corresponds to decay proportional to $t^{-2.5}$, indicative of late-time homogeneous half-space response for the vertical component. Red symbols correspond to positive data whereas blue symbols correspond to negative data.*

Some of the data channels in Figure 5-20 have anomalously low values for all receiver stations. This effect was not random and could not be removed by repeated measurements and averaging. The effect is probably due to interference from 50 Hz noise. The affected channels were not used in the inversion. The decay rate of the corrected vertical component in Figure 5-20 is somewhat slower than the decay for a homogeneous half-space, indicating a decrease of resistivity with depth. The magnitude of the secondary field for early channels corresponds to the response of a half space of around 5,000 Ωm to 6,000 Ωm. The corresponding half-space for late channels would have a resistivity of around 2,000 to 2,500 Ωm.

The inversion results were similar for all receiver stations. The same type of four-layer model as the one used for transmitter loop 1 was used (see section 5.1). The uppermost layer got a resistivity of around 400 Ωm and a thickness of around 23 metres in the inversion. This layer is however not well resolved by the sounding. The inversion output for the second high-resistivity layer was a thickness of 1,250 metres and a resistivity of 15,600 Ωm, whereas the values for the third layer were 3,000 Ωm and 1,170 metres. The resistivity of the third layer was held fixed during the inversion. The resistivity of the substratum was held fixed at 1,000 Ωm during the inversion. The inversion result should however not be regarded as accurate since the ground is indicated to contain a 2D-structure. The fit between field data and model response for station 5 can be seen in Figure 5-21. The station furthest away from the transmitter loop was chosen as it was least affected by the assumed current in the loop. The fit is good except for the noisy channels mentioned above. The forward calculated horizontal components are not shown here. As might be expected there is a poor fit between model response and field data for the horizontal components due to the inferred 2D-structure.

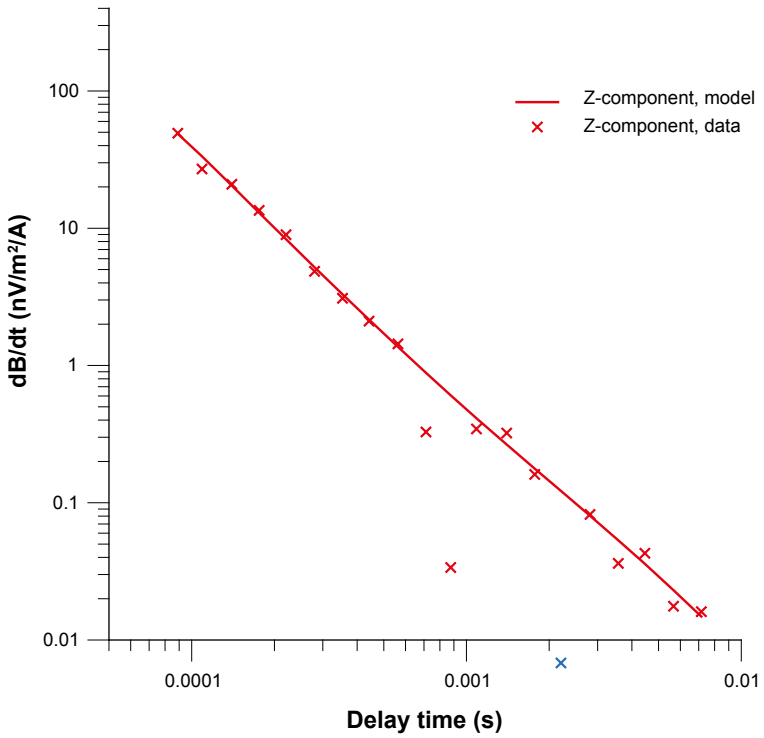

Figure 5-21. *Secondary field, vertical component, transmitter loop 5, station 5. The data have been corrected for the "loop effect". Red symbols correspond to positive data whereas blue symbols correspond to negative data.*

5.6 Transmitter loop 6

Transmitter loop 6 was located near Draknäs, around 10 km south of Forsmark power plant (Figure 1-1). Measurements were made at five stations, of which three were located outside the transmitter loop. The direction of the secondary field was analyzed to investigate the validity of a one-dimensional earth in the interpretation. The secondary field is fairly steep for the stations inside the loop (Figure 5-22) and also quite steep outside the loop, except for station 5. The anomaly at station 5 seems however to be local and might be caused by e.g. fence or a near-surface geologic conductor. The horizontal component is larger outside the loop compared to inside and points almost radially outwards from the loop centre (Figure 5-22). This is consistent with a one-dimensional earth and a horizontally stratified inversion model is therefore justified.

The decay of the vertical component of the secondary field, seen in Figure 5-23, is quite similar for all five stations, except the first channels for station 5. Since the other stations seem unaffected by this anomaly and also that the secondary field of station 5 resembles the other stations for intermediate and late channels, it is reasonable to assume that the anomaly is due to some near-surface phenomenon like a cable or a small geologic conductor. The decay rate of the vertical component is somewhat slower than the decay for a homogeneous half-space, indicating a decrease of resistivity with depth. The magnitude of the secondary field for early channels corresponds to the response of a half space of around 5,500 Ωm. The corresponding half-space for late channels would have a resistivity of around 3,000 Ωm.

The inversion results were similar for all receiver stations, except number 5. The same type of four-layer model as the one used for transmitter loop 1 was used (see section 5.1).

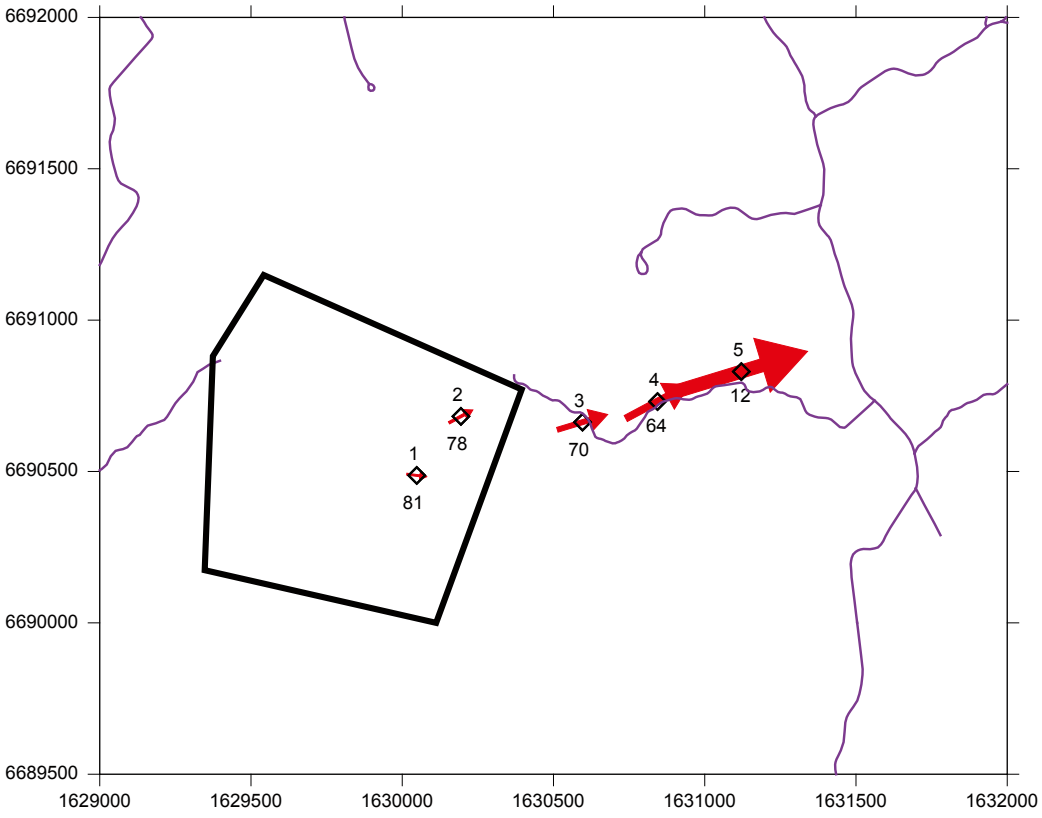

Figure 5-22. *Map showing the positions of transmitter loop 6 (thick black line) and the receiver stations used for that loop (black symbols). The station IDs are shown as labels over the symbols. The labels under the symbols indicate the direction in degrees of the secondary field from the horizontal plane for channel 4 (0.176 ms delay time). The red arrows indicate the inclination and magnitude of the horizontal secondary field for channel 4.*

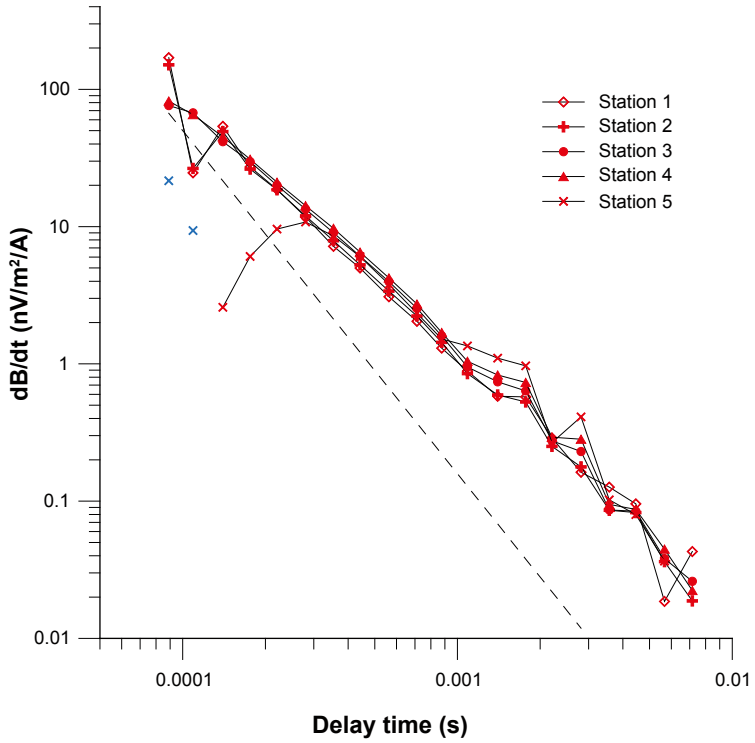

Figure 5-23. *Secondary field decay curves, vertical component, transmitter loop 6. The positions of the stations can be seen in Figure 5-22. The dashed line corresponds to decay proportional to $t^{-2.5}$, indicative of late-time homogeneous half-space response. Red symbols correspond to positive data whereas blue symbols correspond to negative data.*

The uppermost layer got a resistivity of around 370 Ωm and a thickness of around 20 metres in the inversion. This layer is however not well resolved by the sounding. The inversion output for the second high-resistivity layer was a thickness of 600 metres and a resistivity of 16,150 Ωm, whereas the values for the third layer were 3,000 Ωm and 1,750 metres. The resistivity of the third layer was held fixed during the inversion. The resistivity of the substratum was held fixed at 1,000 Ωm during the inversion. The fit between field data and model response for station 2 can be seen in Figure 5-24. The fit is reasonably good except for the first two channels were a residual current in the loop is assumed to have caused noisy data.

The inversions were based on the vertical component of the secondary field. However, forward solutions for the inversion output models can be calculated for the horizontal components. The calculated east component of the secondary field can be compared with field data for station 2 in Figure 5-25. The noise threshold is at around 0.5 nV/m^2/A for the horizontal component, so the late channels should be disregarded. The agreement between field data and model response is quite good for early channels. The north component is of quite low magnitude and is therefore not shown. The layered model seems plausible when the horizontal field is considered.

5.7 Transmitter loop 7

Transmitter loop 7 was located near Lundsvedja, around 16 km south of Forsmark power plant (Figure 1-1). Measurements were made at five stations, of which two were located outside the transmitter loop. The direction of the secondary field was analyzed to investigate the validity of a one-dimensional earth in the interpretation. The secondary field is reversed for two of the stations inside the loop and also the third station shows an anomalous direction (Figure 5-26). Station 4 has a strong horizontal component that points in a direction that is almost perpendicular to what is expected for a layered earth. Metallic fences are present in the area and it is suspected

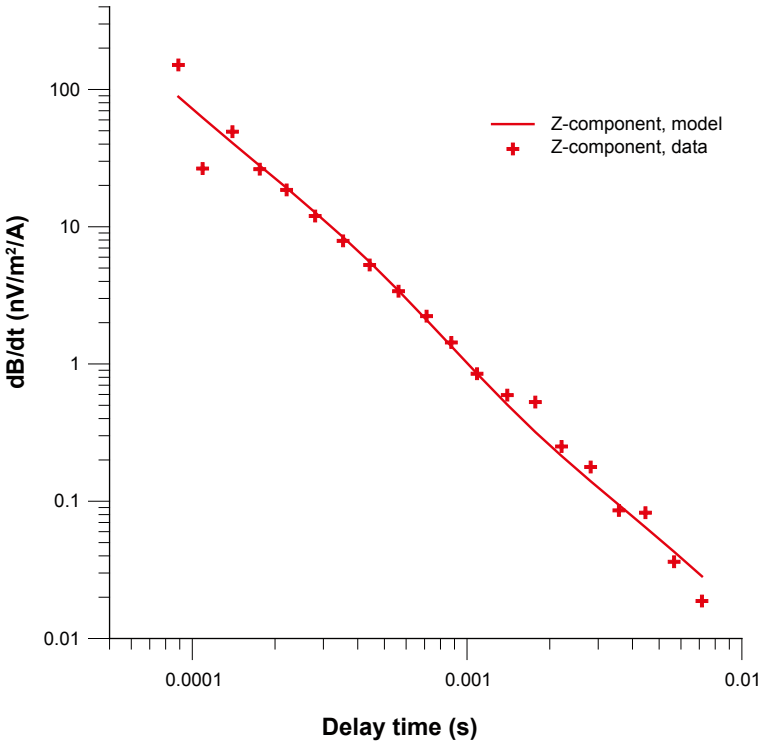

Figure 5-24. *Secondary field, vertical component, transmitter loop 6, station 2.*

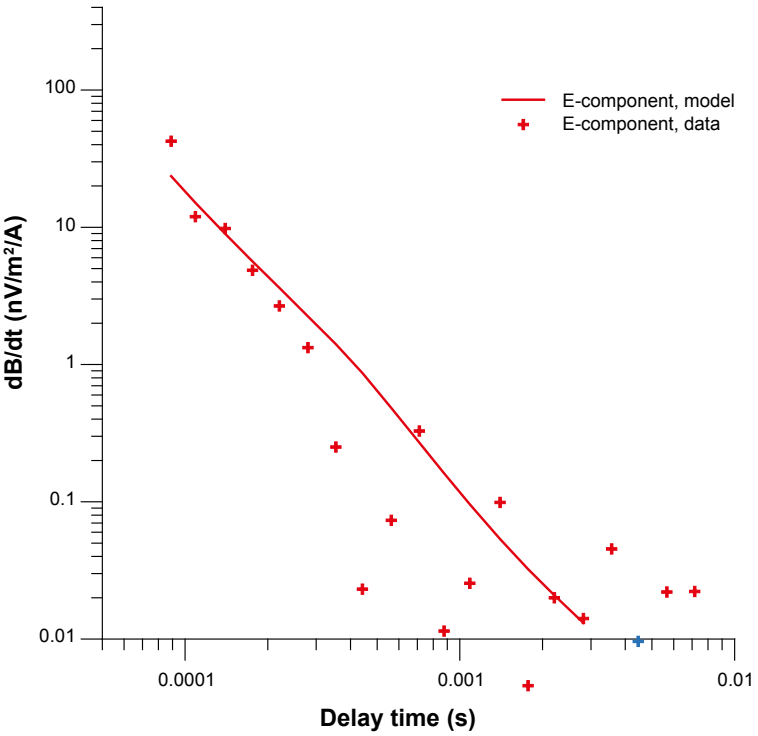

Figure 5-25. *Secondary field, east component, transmitter loop 6, station 2. Red symbols correspond to positive data whereas blue symbols correspond to negative data.*

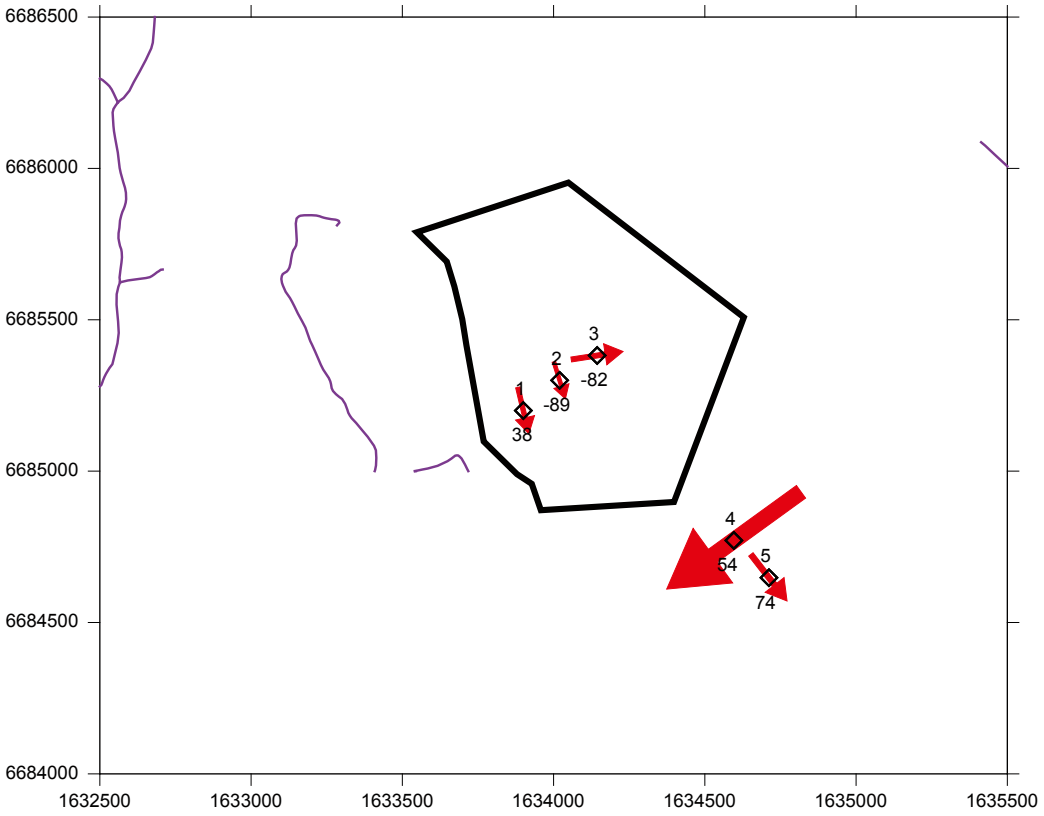

Figure 5-26. *Map showing the positions of transmitter loop 7 (thick black line) and the receiver stations used for that loop (black symbols). The station IDs are shown as labels over the symbols. The labels under the symbols indicate the inclination in degrees of the secondary field from the horizontal plane for channel 4 (0.176 ms delay time). The red arrows indicate the direction and magnitude of the horizontal secondary field for channel 4.*

that these formed closed loops during the survey and hence produced strong secondary fields. Only station 5 has a secondary field that has a direction that is compatible with a layered earth.

The decay of the vertical component of the secondary field, seen in Figure 5-27, shows great dissimilarity between the stations. The data are also quite noisy. No inversion was therefore performed for data from this transmitter loop.

Transmitter loop 7 is located around 6.5 km away from loop 6 but at roughly the same distance away from the sea. A forward response of the inversion model from loop 6 was therefore calculated for loop 7. The only receiver station that gave data that were not severely affected by near-surface objects was station 5. A comparison between the data from this station and the vertical field forward response for the model from loop 6 can be seen in Figure 5-28. The first four channels in the data seem to be affected by some near-surface object. The next three channels show good agreement with the model response. Later channels are however noisy and no meaningful comparison can be made. The corresponding comparison for the horizontal components can be seen in Figure 5-29. Although the E-component is noisy, a good fit to the data can be seen for the first seven channels of the model response. This does not say much about the electrical properties of rock a great depth since no reliable late-time data are available. However, at least the first c. 500 metres of the ground seem to have similar electrical properties at loop 7 as at loop 6.

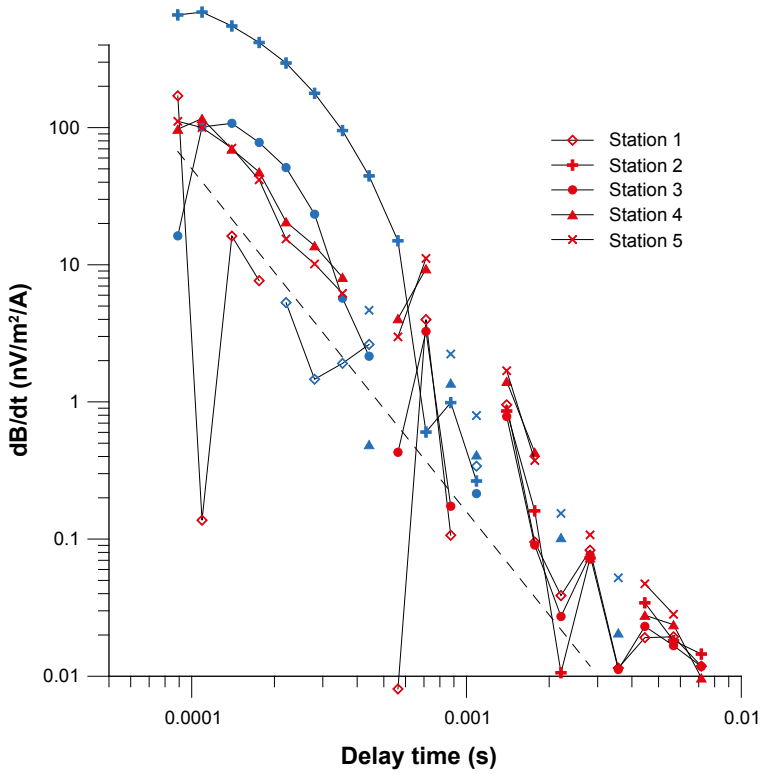

Figure 5-27. *Secondary field decay curves, vertical component, transmitter loop 7. The positions of the stations can be seen in Figure 5-26. The dashed line corresponds to decay proportional to t-2.5, indicative of late-time homogeneous half-space response. Red symbols correspond to positive data whereas blue symbols correspond to negative data.*

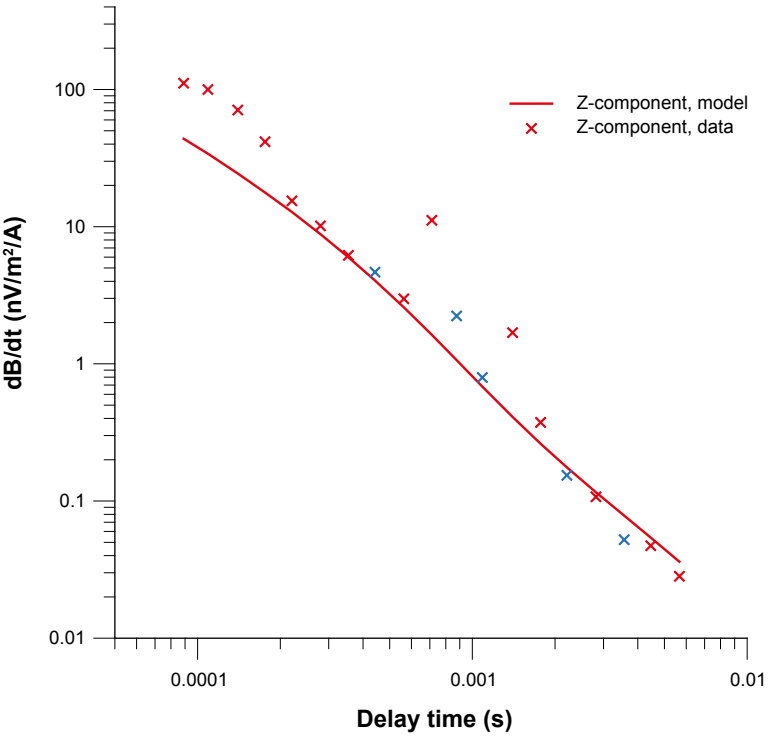

Figure 5-28. *Secondary field, vertical component, transmitter loop 7, station 5. Red symbols correspond to positive data whereas blue symbols correspond to negative data. The solid line corresponds to the system response to the inversion model of loop 6.*

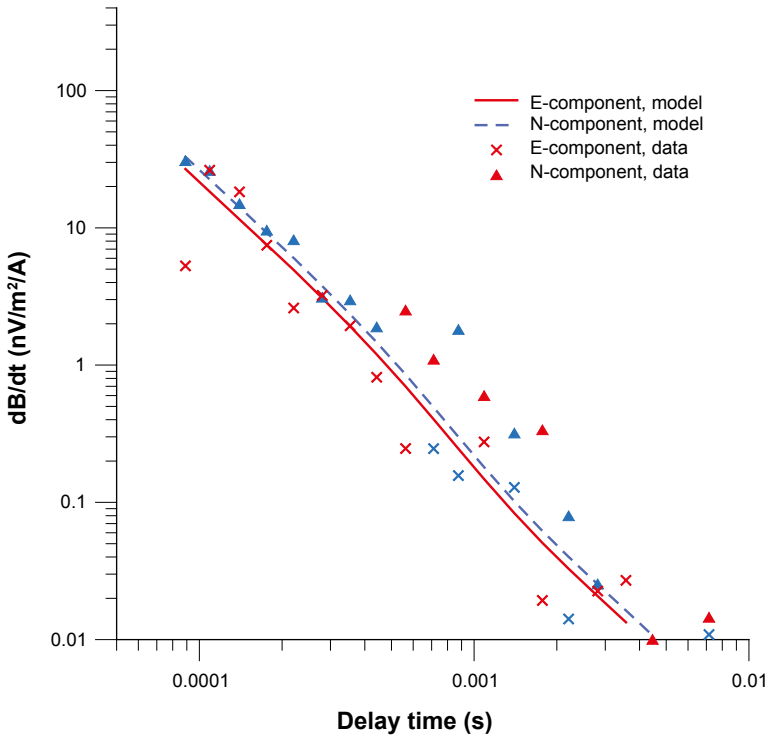

Figure 5-29. *Secondary field, horizontal components, transmitter loop 7, station 5. Red curves/symbols correspond to positive data whereas blue curves/symbols correspond to negative data. The solidand dashed lines corresponds to the system response to the inversion model of loop 6.*

5.8 Resistivity values, discussion

The depth to a conductive layer is a well resolved parameter in the layered models of an electromagnetic sounding. The resistivity values of the various layers are not that well resolved. The four-layer model that was used for inversion modelling was a conceptual one based on known geological conditions (e.g. /2/).

The uppermost layer represents the soil cover. The TEM-sounding data does not provide any constraints for the resistivity of that layer due to its small thickness. However, the layer was still needed since the first channels in general showed lower apparent resistivities compared to e.g. data at around 0.2 to 0.3 ms delay time.

The second layer represents bedrock that is saturated with fresh water (~ 10 to 50 Ωm fluid resistivity). The resistivity of this layer was free during inversion, except for transmitter loop 1. The inversion output varied between 12,400 to 19,700 Ωm. According to available geological maps, all sounding stations were located on granitic rock or other high-resistivity rock types. The model resistivity range for layer two is quite reasonable for such rock types under Swedish geological conditions (e.g. /8/). Electrical soundings with a depth of investigation of a few hundred meters have also estimated the bedrock resistivity around Forsmark to values similar to the ones above /3/. The model resistivity values are also quite similar to median resistivity values measured on samples from the Forsmark candidate area and the regional surroundings /4, 5/. Petrophysical studies /4, 5/ have shown that the resistivity of rocks in the Forsmark area (saturated with fresh water) to a major extent is governed by surface conductivity effects. This means that the resistivity is only weakly dependent upon fluid resistivity under fresh water conditions. It has been suggested that this is the reason why such a layer can appear as having a fairly homogeneous resistivity although an increase in salinity with depth is known to exist /9/.

The third layer in the conceptual model corresponds to bedrock saturated with brackish water (~ 1 to 5 Ωm fluid resistivity). The resistivity of this layer was held constant during inversion since it was poorly constrained by the data. The resistivity was set to 2,500 to 3,500 Ωm. This

range was taken from late time apparent resistivities at stations away from the coast and early time apparent resistivity values from stations close to the coast. The resistivity contrast between layer two and three is around 5 for the different soundings. This is less than the corresponding value for soundings performed around the site investigation at Oskarshamn /10/. The reason for this might be that the transition to a saline environment has a different character in Oskarshamn compared to Forsmark /2, 9/. Data from deep boreholes shows that the salinity increases more or less monotonically with depth in Oskarshamn whereas the salinity reaches a plateau at around 5,000 to 6,000 mg/l in Forsmark and that value is more or less constant for a depth interval of several hundred meters. The TEM soundings cannot resolve the gradual change in fluid resistivity. Instead they experience the transition from surface conductivity domination to pore volume conductivity domination as a layer boundary. The salinity quickly reaches higher values below this boundary in Oskarshamn but not in Forsmark, hence the difference between the resistivity contrasts in the TEM models.

The fourth layer in the conceptual model corresponds to bedrock saturated in saline water (~ 0.2 to 0.8 Ωm fluid resistivity). The resistivity of this layer was held constant during the inversions since it is not well resolved by the data. The resistivity was set to 500 to 1,000 Ωm. The value was based on late time apparent resistivity values for transmitter loops 1 and 2. The model resistivity range is compatible with values obtained from measurements of resistivity on rock samples from Forsmark saturated in saline water /4, 5, 6, 7/.

5.9 Compilation of model results

The results from the seven TEM soundings have been compiled into a simplified model of resistivity distribution in the Forsmark area. It should be noted that several of the model parameters are poorly constrained by the data. This is valid for more or less all layer resistivities. The depth to a conducting layer is better resolved by an electromagnetic sounding. The rather low resistivity contrast between the fresh and brackish water saturated layers will however impose rather large error bounds on the thickness of the former layer. The error bounds varies between the soundings but can be estimated to around ± 30%. The lowermost saline water saturated layer is reliably indicated only for transmitter loops 1 and 2. It is also indicated for loop 3, but at such a large depth that it is poorly determined. The other loops did not indicate this layer and only a possible minimum depth to the interface can be given based on the depth of investigation of the method. That depth is dependent upon the signal-to-noise ratio of the data and also upon the resistivity structure in the ground. A rough estimate would however be that the depth of investigation is around 2,000 to 3,000 metres.

Five of the transmitter loops gave inversion results that can be regarded as quite reliable. The data from loop 7 were severely disturbed by secondary fields from fences and no inversion could be made. Loop 5 was affected by current channelling in a 2D structure to such an extent that layered earth inversion was not a truly valid modelling tool. Loop 5 is located at just a slightly larger distance from the sea compared to loop 2. The two loops are however located on either side of the regional NW-SE trending Forsmark deformation zone. The results for the two loops are significantly different. Rock of high resistivity is only present close to the surface at loop 2 (NE of the deformation zone), whereas high-resistivity rock is indicated to fairy large depths at loop 5 (SW of the deformation zone). The inversion output should not be regarded as accurate for loop 5 since the ground is not one-dimensional. The difference between the two stations is however significant. The two loops are located some distance away from each other and it cannot be excluded that the difference in results is due to this distance. The strong current channelling effects at loop 5 together with the difference in depth to the brackish water interface might however suggest that there is a significant increase in thickness of the fresh water saturated layer towards SW at the Forsmark zone.

Figure 5-30 shows a compilation of the inversion results for the thickness of the fresh water saturated layer. The thickness for loop 1 should be regarded as approximate since such a thin layer becomes transparent to the TEM sounding. The thickness can however not be much larger since it in such a case would affect the data. The value for loop 5 is quite uncertain for

the reasons discussed above. It seems like the inversion has greatly overestimated the depth to lower resistivity rock for this station. The difference in thickness is also quite large between loops 3 and 4. Such a difference would imply a dipping interface, and this is not indicated by the data. However, considering that the error bounds of the layer thickness are quite large it is likely that the difference between the two stations has been overestimated. In such a case it is most likely that the layer thickness for loop 4 is too large. A smaller thickness of 900 m is compatible with the data for this station if the resistivity of the brackish water saturated layer is allowed to increase to around 5,000 Ωm.

A vertical model section has been constructed for the profile marked with a thick dashed line in Figure 5-31. The interpretation of a discontinuity at the Forsmark deformation zone above has been taken into account. The depth to low-resistivity rock has also been assumed to have been over-estimated for transmitter loop 4 in the inversion. The section can be seen in Figure 5-32. Three layers can be seen in the section, although it should be realized that the transition between the layers might be gradual. The top white layer represents fresh water saturated rock with a resistivity of 10,000 Ωm or more. Electrical soundings north of loop 2 /3/, around Lake Bolundsfjärden and a bit further towards west indicate fairly low electrical resistivities close to the surface. This might indicate that the fresh water saturated layer is very thin, or more or less absent in that area. The second, light grey, layer in Figure 5-32 represents bedrock saturated with brackish water and having a resistivity of 2,500 to 3,500 Ωm, possibly slightly higher towards WSW. The thickness of this layer is reasonably well resolved for loops 1 and 2 and less well for loop 3. The lowermost, dark grey, layer in the figure represents bedrock saturated by saline water. The interface between the two bottom layers is indicated to dip towards SE, more or less perpendicular to the profile, at transmitter loops 1 and 2.

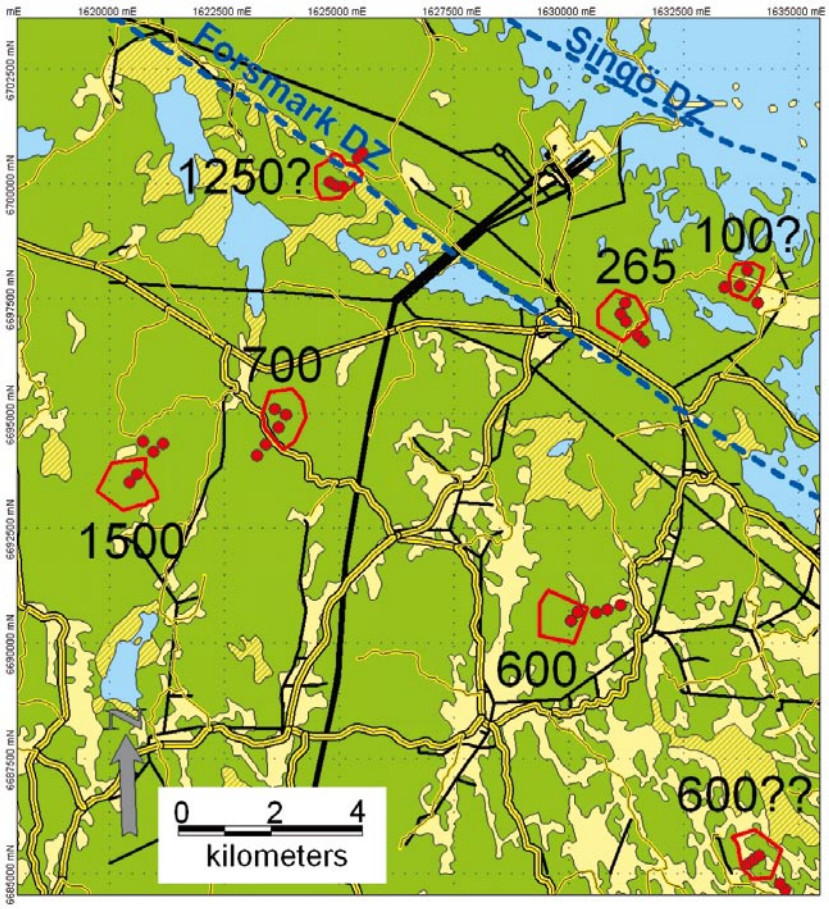

Figure 5-30. *Map showing the inversion output for the thickness in metres of the fresh water saturated bedrock layer. The parameter is poorly determined for three of the stations for reasons explained in the text. The Singö and Forsmark deformation zones are shown with dashed blue lines.*

Figure 5-31. *Map showing the position of the vertical section in Figure 5-32 as a dashed black line. The Singö and Forsmark deformation zones are shown with dashed blue lines.*

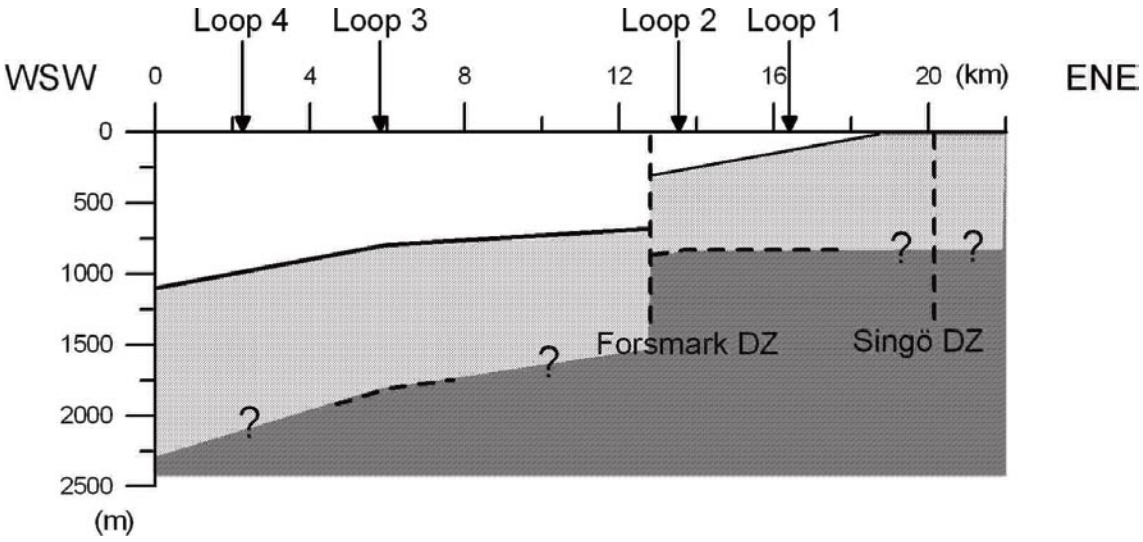

Figure 5-32. *Vertical section showing a generalized interpretation of the sounding data. The layers represents, from top to bottom, rock saturated by fresh, brackish and saline water respectively. The dislocation at the Forsmark deformation zone is mainly based on interpretation of the sounding data from transmitter loop 5 NW of the profile.*

References

/1/ **Kaufman A A, Keller G V, 1983.** Frequency and transient soundings. Elsevier, Amsterdam.

/2/ **Svensk Kärnbränslehantering AB, 2007.** Hydrogeochemical evaluation of the Forsmark site, modelling stage 2.1 – issue report. SKB R-06-69. In prep. Svensk Kärnbränslehantering AB.

/3/ **Thunehed H, Pitkänen T, 2003.** Electric soundings supporting the inversion of helicopterborne EM-data. Forsmark site investigation. SKB P-03-44, Svensk Kärnbränslehantering AB.

/4/ **Isaksson H, Mattsson H, Thunehed H, Keisu M, 2004.** Petrophysical surface data. Stage 2 2003 (including 2002). Forsmark site investigation. SKB P-04-155, Svensk Kärnbränslehantering AB.

/5/ **Mattsson H, Thunehed H, Isaksson H, Kübler L, 2004.** Interpretation of petrophysical data from the cored boreholes KFM01A, KFM02A, KFM03A and KFM03B. Forsmark site investigation. SKB P-04-107, Svensk Kärnbränslehantering AB.

/6/ **Thunehed H, 2005.** Resistivity measurements on samples from KFM01A and KFM02A. Forsmark site investigation. SKB P-05-26, Svensk Kärnbränslehantering AB.

/7/ **Thunehed H, 2005.** Resistivity measurements and determination of formation factors on samples from KFM03A, KFM04A and KFM05A. Forsmark site investigation. SKB P-05-76. Svensk Kärnbränslehantering AB.

/8/ **Thunehed H, 2000.** Mapping and characterisation of Swedish bedrock by DC resistivity and transient-field electromagnetic measurements. Ph.D. thesis. Luleå University of Technology 2000:17.

/9/ **Thunehed H, 2007.** Comparison between measurements of Total Dissolved Solids and Transient Electromagnetic Soundings in the regional model area. Oskarshamn site investigation. SKB P-07-88, Svensk Kärnbränslehantering AB.

/10/ **Thunehed H, Pitkänen T, 2006.** Transient electromagnetic soundings at Laxemar and the regional surroundings. Estimations of depth to saline groundwater. Oskarshamn site investigation. SKB P-06-21, Svensk Kärnbränslehantering AB.